Mathematical Analysis of Macroscopic Models for Slow Dense Granular Flow

Aleksander GRM

April 2007

Department of Mathematics
Univeristy of Kaiserslautern

Mathematical Analysis of Macroscopic Models for Slow Dense Granular Flow

Aleksander GRM

Vom Fachbereich Mathematik
der Technischen Universität Kaiserslautern
zur Verleihung des akademischen Grades
Doktor der Naturwissenschaften
(Doctor rerum naturalium, Dr. rer. nat.)
genehmigte Dissertation

1. Gutacher: Prof. Dr. Axel Klar
2. Gutacher: Prof. Dr. Dr. h.c. em. Helmut Neunzert

Tag der Disputation: 26.04.2007

D 386

Abstract

In this dissertation we present analysis of macroscopic models for slow dense granular flow. Models are derived from plasticity theory with yield condition and flow rule. Corner stone equations are conservation of mass and conservation of momentum with special constitutive law. Such models are considered in the class of generalised Newtonian fluids, where viscosity depends on the pressure and modulo of the strain-rate tensor. We showed the hyperbolic nature for the evolutionary model in 1D and ill-posed behaviour for 2D and 3D. The steady state equations are always hyperbolic. In the 2D problem we derived a prototype nonlinear backward parabolic equation for the velocity and the similar equation for the shear-rate. Analysis of derived PDE showed the finite blow up time. Blow up time depends on the initial condition. Full 2D and antiplane 3D model were investigated numerically with finite element method. For 2D model we showed the presence of boundary layers. Antiplane 3D model was investigated with the Runge Kutta Discontinuous Galerkin method with mesh addoption. Numerical results confirmed that such a numerical method can be a good choice for the simulations of the slow dense granular flow.

To my wife ...

Acknowledgements

I wish to express my deepest appreciation to my supervisor Prof. Axel Klar for his support, guidance and encouragement. I am highly indebted to Prof. em. Helmut Neunzert for giving me the opportunity of doing my Ph.D. in Kaiserslautern and guiding me in the first year.

I am very grateful to Dr. Raimund Wegener for being human department boss. I am particularly indebted to Dr. Robert Feßler for the useful hints, advises and introducing me into the topic of granular flow. I would like to thank the group "Transportforgänge" at Fraunhofer ITWM especially Satyananda Panda, Nicole Marheineke, Jevgenij Jegorovs, Sergiy Pereverzyev, Mathieu Sellier for providing friendly working atmosphere and Alfonso Caiazzo for being a good friend.

The financial support from Franuhofer ITWM, Department of Transport Processes is gratefully acknowledged. Without their support, present work would not have been possible.

Finally, my special thanks go to my wife and my family in particular for their love, support and encouragement.

Contents

Chapter 1

Introduction

A granular material or bulk material can be defined as any material composed of many individual solid particles, irrespective of the particle size. Thus the term granular material embraces a wide variety of materials from the coarsest colliery rubble to the finest icing sugar. The handling of granular materials is of great importance in the industry. We find them in chemical industry, food industry, pharmaceutical industry and geophysical materials.

In this work we will be concentrated in the kinematics, the study of the motion of flowing granular materials. We encounter such flows in geophysical mass flow, such are debris flow, ash flow, volcanic lava flow, dense landslides (grain size 1cm-1m), flows in pharmaceutical industry (grain size 0.1mm), flows in food industry (grain size 1mm-10mm), etc.

The analysis of stress and velocity distributions is based on principles laid down in the eighteenth century by Coulomb [Cou76] and which have been developed by the soil mechanicists. The emphasis in our case is however different. Whereas in soil mechanics the main objective is to prevent movement in the soil, the converse is true in bulk solids handling flow situation.

Modelling the flow of granular materials has been extensively studied through the use of continuum mechanics, which is also the approach in this work. Using this approach, one formulates governing equations for the stress and velocity fields by coupling the equations of conservation of mass and linear momentum with appropriate constitutive laws that govern the initiation of failure and the rules applicable to the flow of the granular material subsequent to its failure.

Similar to fluid flow, where several characteristic numbers, like Froude number, Reynolds number, etc., can be used to characterise the qualitative flow behaviour, the various powder regimes can be represented as a function of a dimensionless shear rate $\dot{\gamma}^* = \dot{\gamma}\sqrt{d_p/g}$ which contains a gravitational term g and a particle size

d_p (see [TMT02]). Based on such a characterisation, one has the following three different regimes:

- **Quasi-static regime**

  This regime is valid when the flow is slow enough so that any movement between two static states can be neglected. In this case the static equilibrium equation can be applied. With this approach only stress and condition of the onset of flow can be computed, while no flow field can be predicted which circumscribes the range of applications of this approach. There is a large number of analytical and numerical solutions to this case and an important number of literature devoted to this regime; see for instance [Ned92], [GM01].

- **Slow and frictional regime**

  In this regime the frictional forces between particles are predominant, so the inertial effect is added to the static equations as well as the consideration of continuity beside a yield condition. The first model invoking a flow rule was introduced by Drucker & Prager [DP52]. An extensive analysis of such models was performed by the group of D. G. Schaeffer (i.e. [SSP90]). This regime is very important since it can be used for modelling a wide range of practical phenomena and industrial applications. However, for the serious challenges which arise in this regime, for instance ill-posed partial differential equations (dynamic Eq. [Sch87], steady Eq. [SSW06, MS04]) and the prediction of stress fluctuations [Han05], there is still a lack of fundamental research so that dealing with these problems requires a multidisciplinary treatment. Our contribution has the goal of supporting this part by analytical and numerical investigation which will be described in the subsequent sections.

- **Intermediate and rapid granular regimes**

  For the intermediate regime, additional to inter-particle friction energy, collision energy is also important. For the rapid regime, the short particle-particle contacts are important while frictional forces are neglected. This regime is often described via kinetic models and will not be treated here. It was reported here just to have a complete view on the different regimes of granular flow (see [TMT02] for more details).

The problem of modelling fully developed slow granular flows using continuum mechanics is, and continues to be, both complex and challenging. There is a

general agreement that the stress fields within granular flows can be described by coupling the equations of linear momentum with the yield condition. However, there is a little or no agreement as to how the equations for the velocity fields, that describe the deformation of fully developed flows, should be formulated, or weather this equations should be mathematically well-posed or ill-posed. The constitutive assumption, perhaps most widely employed is Saint-Venant's principle, which is also referred to as the coaxiality condition. This condition states that the principal axes of the stress and strain-rate tensors should coincide. Drucker and Prager [DP52] were the first to formally adopt this principle for the study of the mechanics of granular materials. The condition of coaxiality must hold by virtue of material isotropy, and the strain-rate tensor only depend on the Cauchy stress tensor.

While the work of Drucker and Prager marks the resurgence of the application of plasticity theories to mechanics of soils, these developments have limitations. Firstly, the theory predicts that all granular flows are accompanied by dilation or volume change, notably volume expansions, whereas in fact loose packed granular materials contract (consolidate) upon shearing and others undergo isohoric or volume-preserving deformations. Even in situations for which dilation is appropriate, the predicted magnitude of volume increase is far in excess of those observed in real materials. The second limitation is that for cohesion less materials, the theory predicts that the rate of specific mechanical energy dissipation is zero (with increase of flow rate there is no change in resistance – consume of the power is equivalent), which is clearly unrealistic. More sophisticated approaches attempt to overcome these difficulties by either including work hardening/softening theories, or to incorporate of flow rules that are non-associated. In the former category of models, the yield condition varies with a state parameter such as the density. For the work hardening/softening models, the characteristics (in hyperbolic meaning) for the stress and velocity fields do not coincide, contrary what is comonly observed in experiments. This leads to the adoption of non-associated flow rules.

By abandoning the assumption of coaxiality, an alternative family of models has been derived based on a kinematic hypothesis involving the concept of shearing motion parallel to surface, rotation of that surface, and dilation and contraction normal to the surface. One such model is the double shering model original proposed by Spencer [Spe64] for incompressible flows and extended for dilatant materials by Mehrabadi & Cowin [Spe64] and Butterfield & Harkens [MC72]. In this theory the characteristic curves for the stress and velocity fields coincide, and every deformation is assumed to consist of simultaneous shearing along the two families of stress characteristics. To reiterate, an important advantage of the

double shearing theory over the previous coaxial theories is that it retains the assumption of slip occurring along the stress characteristics, but does not give rise to unusually high level of dilatancy. On the other hand, there are experiments, which are not consistent with Spencer's double shearing theory.

Research in this area must recognise the fact that there is a little possibility for developing a mathematical theory of granular media for all eventualities; the materials are real and the circumstances diverse. At this moment no single theory is clearly most applicable for describing the fully developed flow of real granular materials.

In addition to the problems raised above, a major unresolved questions with Spencer's double-shearing theory, and most other plasticity based theories for fully developed granular flow, is that the equations are linearly ill-posed in the sense that small perturbations to existing solutions may result in solutions that grow exponentially in time (see e.g. [Spe86], [Sch87], [PS87], [Har01]). However, ill-posedness in itself is not necessarily an undesirable property for equations that describe deformations of granular materials. In fact, it is well known that under certain circumstances granular materials exhibit unstable behaviour, in which case it is quite plausible that ill-posedness should be a norm. An example is onset of shear-banding.

By the author judge, there is a chance in a multi-physics model, which describe domain of well-posed problem by one model and the domain of ill-posed problem with another model, which is well-posed under actual circumstances. However, there are many question, like how to couple models, who evolves the boundary, etc.

In this thesis, we restrict our attention to the plasticity theory models. In the first chapter we derive the compressible associated granular flow model which we name as Slow Dense Granular Flow (SDGF) model. In the first part of the thesis, we analytically investigate SDGF model. We show hyperbolic nature of the 1D model and the ill-posed behaviour for higher dimensions. The second part of the thesis numerically investigates two different models of granular flow. The first model is the same as in part one. Numerical analysis detects the same behaviour as was predicted by the analysis in the part one. This confirms, that the approximations we did in the part one are in a good agreement with the full model. The second model [Sch92] includes the effects of elasticity. It is confined in a special geometry, the so called anti plane model. This model was derived with the motivation to study onset of shear-bands. It is also a testing model for the new numerical algorithms for granular flows. We used Discontinuous Galerkin-Runge Kutta finite element method with mesh adaption to solve anti

plane shear model. Numerical results are in a good agreement compared to the one in the work of Garaizar & Trangenstein [GT98].

Chapter 2

Physical Model for Slow Dense Granular Flow (SDGF)

In this chapter we will derive a physical model for the description of slow dense granular flow (SDGF). For this purpose, we assume the granular media to be a continuum. We will state down conservation laws and provide a constitutive relation to close the model.

2.1 Notation

We study the SDGF as a continuum media. Therefore, we have to describe it in the language of continuum mechanics. In this section we will prepare the ground notations for the model derivation and its analysis. Vector and tensor notations are written in the Appendix A. For detailed description reader should consult the standard text in Continuum Mechanics ([TT65], [MH92], [Gur81],etc.)

2.1.1 Continuum body

Definition 2.1.1 (Configuration, Motion, Deformation)**.** A ***body*** $\mathscr{B}$ is a set whose elements can be put into one-to-one correspondence with points of a simply connected domain $\mathcal{B}$ in three-dimensional Euclidean space $\mathbb{R}^3$. We shall refer to such a region as a ***configuration*** of the body. The elements of $\mathscr{B}$ are called ***particles*** (or ***material points***). According to this definition, we have an invertible mapping

$$\boldsymbol{\kappa} : \mathscr{B} \times \mathbb{R}^+ \to \mathcal{B} \subset \mathbb{R}^3,$$

which associates to each element $P \in \mathscr{B}$ at time t, a point in $\mathcal{B}$, say $\boldsymbol{\kappa}(P,t)$. The dependence on time (here denoted by t) is included because during a ***motion*** the body changes its configuration with time. In order to provide a natural description of the motions undergone by $\mathscr{B}$, an arbitrary (but fixed) configuration is chosen as ***reference configuration*** and this will be denoted by $\mathcal{B}_r$. For the sake of simplicity, we choose

$$\mathcal{B}_r := \boldsymbol{\kappa}(\mathscr{B}, 0).$$

On the other hand, the configuration of $\mathscr{B}$ at time t is denoted by

$$\mathcal{B}_t := \boldsymbol{\kappa}(\mathscr{B}, t),$$

and this represents the ***current configuration*** of the body (which obviously depends on time). We will denote the upper-case symbols related to the reference configuration and the lower-case symbols to the current configuration. By letting

$$\boldsymbol{X} := \boldsymbol{\kappa}(P, 0) \quad \text{and} \quad \boldsymbol{x} := \boldsymbol{\kappa}(P, t),$$

we can then eliminate P from these two relations,

$$\boldsymbol{x} = \boldsymbol{\kappa}(\boldsymbol{\kappa}^{-1}(\boldsymbol{X}, 0), t) \equiv \boldsymbol{\phi}(\boldsymbol{X}, t),$$

where $\boldsymbol{\phi}(\cdot,\cdot)$ is defined by the right-hand equality above. This mapping is evidently bijective and we assume that it has all the differentiability properties required in what follows. In continuum mechanics, $\boldsymbol{\phi}$ is known as the ***motion*** of the body $\mathscr{B}$. At fixed time, $\boldsymbol{\phi}$ defines the ***deformation*** of the body from $\mathcal{B}_r$ to $\mathcal{B}_t$, while at a fixed (generic) point $\boldsymbol{X}$, $\boldsymbol{\phi}$ describes the ***trajectory*** of the point.

Definition 2.1.2 (Motion)**.** The mapping $\boldsymbol{\phi}$ is the mapping from reference configuration (or body configuration) frame $\mathcal{B}_r$ to the current configuration (or spatial) frame $\mathcal{B}_t$

$$\boldsymbol{\phi}(\cdot, t) : \mathcal{B}_r \to \mathcal{B}_t.$$

Problems in continuum mechanics may be formulated either employing $(\boldsymbol{X}, t)$ as independent variables in the so-called ***material*** or ***Lagrangian description*** or $(\boldsymbol{x}, t)$ as independent variables in the so-called ***spatial*** or ***Eulerian description***.

Definition 2.1.3 (Rigid motion)**.** A motion of a body $\mathscr{B}$ is said to be ***rigid*** if the distance between the points occupied by every pair of particles is invariable. For such motions we have

$$\boldsymbol{x} = \boldsymbol{\phi}(\boldsymbol{X}, t) = \mathbf{Q}(t)\boldsymbol{X} + \boldsymbol{c}(t), \tag{2.1}$$

where $\mathbf{Q}(t)$ is a proper orthogonal tensor, $\mathbf{Q}^{\mathsf{T}}\mathbf{Q} = \mathbf{I}$, (which may depend on t) and $\boldsymbol{c}(t)$ a given vector (which may depend on t as well). Note that

$$\boldsymbol{X} = \boldsymbol{\phi}^{-1}(\boldsymbol{x}, t) = \mathbf{Q}^{\mathsf{T}}(t)(\boldsymbol{x} - \boldsymbol{c}(t)). \tag{2.2}$$

Remark. It can be proved that every rigid motion can be expressed in the form (2.1). Note that $\boldsymbol{c}(t)$ represents a ***translation***, and $\mathbf{Q}(t)$ a ***rotation***.

2.1.2 Velocity and Acceleration fields

The velocity and acceleration fields of a continuum body are the primary kinematic fields used in describing its motion. Since every continuum body is endowed with two different types of configurations (***material*** and ***spatial***), the velocity and the acceleration fields admit two distinct representations.

Definition 2.1.4 (Velocity and Acceleration)**.**

(1) The ***velocity*** $\boldsymbol{V}$ of a particle $P \in \mathcal{B}$ is

$$\boldsymbol{V}(\boldsymbol{X}, t) := \frac{\partial \boldsymbol{\phi}(\boldsymbol{X}, t)}{\partial t}, \tag{2.3}$$

where $\boldsymbol{X}$ is the position of $P \in \mathcal{B}_r$. This is the rate of change of position of P in the Lagrangian description. It is important to notice that the Lagrangian velocity $\boldsymbol{V}(\boldsymbol{X}, t)$ is a ***two-point order-one*** tensor field *i.e.*, the domain is in material frame $\mathcal{B}_r$ but the range is in tangent space of spatial frame $\mathbb{T}\mathcal{B}_t$.

The corresponding vector field in Eulerian description is

$$\begin{aligned} \boldsymbol{v}(\boldsymbol{x}, t) &:= (\boldsymbol{V} \circ \boldsymbol{\phi}^{-1})(\boldsymbol{x}, t) \\ &= \left.\frac{\partial \boldsymbol{\phi}(\boldsymbol{X}, t)}{\partial t}\right|_{\boldsymbol{X} = \boldsymbol{\phi}^{-1}(\boldsymbol{x}, t)} \\ &\equiv \boldsymbol{V}(\boldsymbol{\phi}^{-1}(\boldsymbol{x}, t)). \end{aligned} \tag{2.4}$$

(2) The ***acceleration*** $\boldsymbol{A}$ of a particle $P \in \mathcal{B}$ is

$$\boldsymbol{A}(\boldsymbol{X}, t) := \frac{\partial^2 \boldsymbol{\phi}(\boldsymbol{X}, t)}{\partial t^2} \tag{2.5}$$

Note that this is a Lagrangian field; its Eulerian counterpart is

$$\begin{aligned} \boldsymbol{a}(\boldsymbol{x}, t) &:= (\boldsymbol{A} \circ \boldsymbol{\phi}^{-1})(\boldsymbol{x}, t) \\ &= \left. \frac{\partial^2 \boldsymbol{\phi}(\boldsymbol{X}, t)}{\partial t^2} \right|_{\boldsymbol{X} = \boldsymbol{\phi}^{-1}(\boldsymbol{x}, t)} \\ &\equiv \boldsymbol{A}(\boldsymbol{\phi}^{-1}(\boldsymbol{x}, t)). \end{aligned} \tag{2.6}$$

Remark. Above, $\boldsymbol{X} \in \mathcal{B}_r$ and $\boldsymbol{x} \in \mathcal{B}_t$ represent the position vectors of the (same) particle P in the reference and the current configurations, respectively. Obviously, velocities and accelerations in both coordinate systems must be the same.

Next, we introduce the concept of ***material time derivative***. To understand this important operation, let us imagine the following situation: suppose that a certain field (scalar, vectorial or tensorial) is defined over the body, and we wish to know its rate of change as would be recorded at a given particle $\boldsymbol{X}$ during the motion. There are two situations to consider:

(1) ***Material fields***: This is the easy case. In the material description, the independent variables are $\boldsymbol{X}$ and t, so all we have to do is take the partial derivative of the given field with respect to t. For example, if $\varphi(\boldsymbol{X}, t)$ is a material scalar field, then

$$\dot{\varphi} \equiv \frac{\mathrm{D}\varphi}{\mathrm{D}t} := \frac{\partial \varphi(\boldsymbol{X}, t)}{\partial t}$$

where the first two equalities indicate the standard notation for the material derivative. We can similarly calculate material time derivatives of Lagrangian vector and tensor fields.

(2) ***Spatial fields***: This case requires some careful thinking: we must calculate the partial derivative, with respect to time, of the material description of the field under consideration, keeping $\boldsymbol{X}$ fixed. In this process we need to remember the chain rule of partial derivation. Let $\varphi(\boldsymbol{x}, t)$ be a spatial scalar field. By definition, the material time derivative of this Eulerian field is

$$\dot{\varphi} \equiv \frac{\mathrm{D}\varphi}{\mathrm{D}t} := \left.\frac{\partial \varphi(\boldsymbol{\phi}(\boldsymbol{X},t),t)}{\partial t}\right|_{\boldsymbol{X}=\boldsymbol{\phi}^{-1}(\boldsymbol{x},t)} \tag{2.7}$$

The same definition applies for vector or tensor fields (with the obvious changes, of course). In practice, the material time derivative can be calculated as follows. First, we need to convert our field into its material representation by using $\boldsymbol{x} = \boldsymbol{\phi}(\boldsymbol{X},t)$,

$$\varphi(\boldsymbol{x},t) = \varphi(\boldsymbol{\phi}(\boldsymbol{X},t),t) = \varphi(\phi_1(\boldsymbol{X},t),\phi_2(\boldsymbol{X},t),\phi_3(\boldsymbol{X},t),t).$$

Differentiation with respect to t, keeping $\boldsymbol{X}$ fixed (constant), leads to

$$\begin{aligned}\frac{d\varphi(\boldsymbol{\phi}(\boldsymbol{X},t),t)}{dt} = &\frac{\partial \varphi(\boldsymbol{\phi}(\boldsymbol{X},t),t)}{\partial x_1}\frac{\partial \phi_1(\boldsymbol{X},t)}{\partial t} \\ &+ \frac{\partial \varphi(\boldsymbol{\phi}(\boldsymbol{X},t),t)}{\partial x_2}\frac{\partial \phi_2(\boldsymbol{X},t)}{\partial t} \\ &+ \frac{\partial \varphi(\boldsymbol{\phi}(\boldsymbol{X},t),t)}{\partial x_3}\frac{\partial \phi_3(\boldsymbol{X},t)}{\partial t} \\ &+ \frac{\partial \varphi(\boldsymbol{\phi}(\boldsymbol{X},t),t)}{\partial t},\end{aligned}$$

which can be conveniently written, by using the summation convention, as

$$\frac{d\varphi(\boldsymbol{\phi}(\boldsymbol{X},t),t)}{dt} = \frac{\partial \varphi(\boldsymbol{\phi}(\boldsymbol{X},t),t)}{\partial x_i}\frac{\partial \phi_i(\boldsymbol{X},t)}{\partial t} + \frac{\partial \varphi(\boldsymbol{\phi}(\boldsymbol{X},t),t)}{\partial t}, \tag{2.8}$$

The last step consists in returning to the spatial description, by making the substitution $\boldsymbol{X} = \phi^{-1}(\boldsymbol{x},t)$ in (2.8), which leads to

$$\left.\frac{d\varphi(\boldsymbol{\phi}(\boldsymbol{X},t),t)}{dt}\right|_{\boldsymbol{X}=\boldsymbol{\phi}^{-1}(\boldsymbol{x},t)} = \frac{\partial \varphi(\boldsymbol{\phi}(\boldsymbol{X},t),t)}{\partial x_i} v_i(\boldsymbol{x},t) + \frac{\partial \varphi(\boldsymbol{\phi}(\boldsymbol{X},t),t)}{\partial t}$$

where $v_i(\boldsymbol{x},t)$ are the components of the Eulerian velocity field defined in (2.4). The right hand-side of this last relation can be written compactly in the form

$$\boldsymbol{v}(\boldsymbol{x},t)\cdot\nabla\varphi(\boldsymbol{x},t) + \frac{\partial \varphi(\boldsymbol{x},t)}{\partial t}.$$

To summarise, we have proved the important formula

$$\dot{\varphi} \equiv \frac{\mathrm{D}\varphi}{\mathrm{D}t} = \boldsymbol{v}(\boldsymbol{x},t)\cdot\nabla\varphi(\boldsymbol{x},t) + \frac{\partial\varphi(\boldsymbol{x},t)}{\partial t}. \tag{2.9}$$

For an Eulerian vector field a similar result can be established as follows. According to the definition (2.7), the material time derivative of such a vector field $\boldsymbol{u}(\boldsymbol{x},t)$ is

$$\dot{\boldsymbol{u}} \equiv \frac{\mathrm{D}\boldsymbol{u}}{\mathrm{D}t} := \left.\frac{\partial \boldsymbol{u}(\boldsymbol{\phi}(\boldsymbol{X},t),t)}{\partial t}\right|_{\boldsymbol{X}=\boldsymbol{\phi}^{-1}(\boldsymbol{x},t)} \tag{2.10}$$

Assuming that the components of $\boldsymbol{u}(\boldsymbol{x},t)$ are $u_i(\boldsymbol{x},t)$ (scalar fields), by using the same type of arguments as above, we find that

$$\frac{du_i(\boldsymbol{\phi}(\boldsymbol{X},t),t)}{dt} = \frac{\partial u_i(\boldsymbol{x},t)}{\partial x_j}v_j(\boldsymbol{x},t) + \frac{\partial u_i(\boldsymbol{x},t)}{\partial t},$$

and thus we get compact relation for an Eulerian vector field

$$\dot{\boldsymbol{u}} \equiv \frac{\mathrm{D}\boldsymbol{u}}{\mathrm{D}t} = \boldsymbol{v}(\boldsymbol{x},t)\cdot\nabla\boldsymbol{u}(\boldsymbol{x},t) + \frac{\partial\boldsymbol{u}(\boldsymbol{x},t)}{\partial t}. \tag{2.11}$$

2.1.3 The Deformation Gradient

Definition 2.1.5. The ***deformation gradient tensor*** F is the derivative of the mapping $\boldsymbol{\phi}$

$$\begin{aligned}\mathsf{F}(\boldsymbol{X},t) &:= \mathrm{D}\boldsymbol{\phi}\\ &= \nabla|_{\boldsymbol{X}}\,\boldsymbol{\phi}(\boldsymbol{X},t)\\ &= \nabla|_{\boldsymbol{X}}\,\boldsymbol{x}.\end{aligned} \tag{2.12}$$

The deformation gradient F is ***two-point*** tensor because it involves points in 2 different configurations (it maps vectors in $\mathcal{B}_r$ onto vectors in $\mathcal{B}_t$). The component representation of the deformation gradient tensor is

$$\mathsf{F}(\boldsymbol{X},t) = \frac{\partial\phi_i}{\partial p_\alpha}\,\boldsymbol{e}_i\otimes\boldsymbol{E}_\alpha = \mathsf{F}_{i\alpha}\,\boldsymbol{e}_i\otimes\boldsymbol{E}_\alpha, \qquad i,\alpha = 1,2,3.$$

where $\boldsymbol{E}_\alpha$ are basis vectors in material frame, $\boldsymbol{e}_i$ are basis vectors in spatial frame. Since $\boldsymbol{\phi}(\cdot,t) : \mathcal{B}_r \to \mathcal{B}_t$ is one-to-one for all $t > 0$, it has an inverse, $\boldsymbol{\phi}^{-1}(\cdot,t) : \mathcal{B}_t \to \mathcal{B}_r$, so we can define

$$\begin{aligned}\mathbf{F}^{-1}(\boldsymbol{X},t) &:= \mathsf{D}\boldsymbol{\phi}^{-1} \\ &= \nabla|_{\boldsymbol{x}}\,\boldsymbol{\phi}^{-1}(\boldsymbol{x},t)) \\ &= \nabla|_{\boldsymbol{x}}\,\boldsymbol{X}.\end{aligned} \tag{2.13}$$

with the component representation

$$\mathbf{F}(\boldsymbol{X},t)^{-1} = \frac{\partial \phi_i^{-1}}{\partial p_\alpha}\,\boldsymbol{e}_i \otimes \boldsymbol{E}_\alpha = \mathsf{F}^{-1}_{i\alpha}\,\boldsymbol{e}_i \otimes \boldsymbol{E}_\alpha, \qquad i,\alpha = 1,2,3.$$

The next relation then holds

$$\mathbf{F}\mathbf{F}^{-1} = \mathbf{F}^{-1}\mathbf{F} = \mathbf{I}.$$

Note that since $\mathbf{F}$ is invertible, it then follows that

$$J = J(\boldsymbol{X},t) := \mathsf{det}\mathbf{F}(\boldsymbol{X},t) \neq 0. \tag{2.14}$$

Since $\mathbf{F} = \mathbf{I}$ in the reference configuration (at time $t = 0$) and $\mathsf{det}\mathbf{F}$ is a smooth real-valued mapping which does not vanish, we deduce that

$$J(\boldsymbol{X},t) > 0, \quad \forall \boldsymbol{X} \in \mathcal{B}_r, t > 0$$

J is known as the ***Jacobian of the motion***.

Definition 2.1.6 (Isohoric motion)**.** If a motion $\boldsymbol{\phi}$ is such that there is no change in volume, then the motion is said to be ***isochoric***. In that case

$$J(\boldsymbol{X},t) = 1, \quad \forall \boldsymbol{X} \in \mathcal{B}_r, t > 0.$$

2.1.4 Curves, Surfaces and Volumes

Consider a ***material curve*** in the reference configuration,

$$\boldsymbol{X} = \boldsymbol{\Gamma}(s), \quad s \in [a,b] \subset \mathbb{R}, \tag{2.15}$$

where s denotes a parametrisation of this curve. During a certain motion $\boldsymbol{X}$, this material curve deforms into a spatial curve,

$$\boldsymbol{x} = \boldsymbol{\gamma}(s,t), \quad s \in [a,b] \subset \mathbb{R}.$$

We can write

$$\boldsymbol{x} = \boldsymbol{\gamma}(s,t) = \boldsymbol{\phi}(\boldsymbol{\Gamma}(s),t), \tag{2.16}$$

and then introduce the so-called ***material tangent vector*** at $\boldsymbol{X} \in \mathcal{B}_r$ (or material line element)

$$\boldsymbol{P} := \frac{d\boldsymbol{\Gamma}(s)}{ds},$$

and the spatial tangent vector at $\boldsymbol{x} \in \mathcal{B}_t$ (or spatial line element),

$$\boldsymbol{p} := \frac{d\boldsymbol{\gamma}(s,t)}{ds}.$$

Taking the derivative of (2.16) with respect to s results in

$$\frac{d\gamma_i(s,t)}{ds} = \frac{\partial \phi_i}{\partial X_\alpha}\frac{d\Gamma_\alpha(s)}{ds} \rightarrow \frac{d\boldsymbol{\gamma}(s,t)}{ds} = \nabla|_{\boldsymbol{X}}\,\boldsymbol{\phi}(\boldsymbol{X},t)\frac{d\boldsymbol{\Gamma}(s)}{ds}$$

thus leading us to the important relations

$$\boldsymbol{p} = \mathbf{F}\boldsymbol{P}, \quad \text{and} \quad \boldsymbol{P} = \mathbf{F}^{-1}\boldsymbol{p}. \tag{2.17}$$

Relations (2.17) are sometimes written

$$d\boldsymbol{x} = \mathbf{F}d\boldsymbol{X}, \quad \text{and} \quad d\boldsymbol{X} = \mathbf{F}^{-1}d\boldsymbol{x}. \tag{2.18}$$

Remark. From (2.17) we clearly see, that $\mathbf{F}$ is a two point tensor. It maps line elements in $\mathcal{B}_r$ to the line elements in $\mathcal{B}_t$. In the language of modern differential geometry the living space of line elements is named ***tangent space*** and denoted by $\mathbb{T}$. Tangent space is always associated with the supporting point in our case point in reference and current configuration. For the material line element we have $\boldsymbol{P} \in \mathbb{T}_{\boldsymbol{X}}\mathcal{B}_r$ and the spatial line element $\boldsymbol{p} \in \mathbb{T}_{\boldsymbol{x}}\mathcal{B}_t$, then follows that the deformation gradient is a mapping

$$\mathbf{F} : \mathbb{T}_{\boldsymbol{X}}\mathcal{B}_r \rightarrow \mathbb{T}_{\boldsymbol{x}}\mathcal{B}_t.$$

Our next objective is to find out how the element of ***area*** and the element of ***volume*** change when moving from $\mathcal{B}_r$ to $\mathcal{B}_t$.

Consider a surface $\mathcal{S}_r \subset \mathcal{B}_r$ which deforms into the surface $\mathcal{S}_t \subset \mathcal{B}_t$ (that is, $\mathcal{S}_t = \boldsymbol{\phi}(\mathcal{S}_r, t)$). Let $\boldsymbol{X} \in \mathcal{S}_r$ and $\boldsymbol{x} \in \mathcal{S}_t$ be its image through $\boldsymbol{\phi}$. Let $d\boldsymbol{X}$ and $d\boldsymbol{Y}$ be material line elements based at $\boldsymbol{X}$, and let $d\boldsymbol{x}$ and $d\boldsymbol{y}$ be their images through the deformation.

If F denotes the deformation gradient, then

$$d\boldsymbol{x} = \mathsf{F}d\boldsymbol{X}, \quad d\boldsymbol{y} = \mathsf{F}d\boldsymbol{Y}. \tag{2.19}$$

By definition, the elements of area in the reference and current configurations, respectively, are given by

$$\begin{aligned} dA :=& \|d\boldsymbol{X} \wedge d\boldsymbol{Y}\|, \\ da :=& \|d\boldsymbol{x} \wedge d\boldsymbol{y}\|. \end{aligned} \tag{2.20}$$

The referential element of volume dV at $\boldsymbol{X} \in \mathcal{B}_r$ is by definition

$$dV := d\boldsymbol{X} \cdot (d\boldsymbol{Y} \wedge d\boldsymbol{Z}) \equiv [d\boldsymbol{X}, d\boldsymbol{Y}, d\boldsymbol{Z}]. \tag{2.21}$$

During the motion, dV is carried into an element of volume dv at $\boldsymbol{x} \in \mathcal{B}_t$, whose definition is

$$dv := d\boldsymbol{x} \cdot (d\boldsymbol{y} \wedge d\boldsymbol{z}) \equiv [d\boldsymbol{x}, d\boldsymbol{y}, d\boldsymbol{z}]. \tag{2.22}$$

Remembering (2.19) with a help of (2.21) and (2.22) we can relate the two elements of volume

$$\begin{aligned} dv &= [\mathsf{F}d\boldsymbol{X}, \mathsf{F}d\boldsymbol{Y}, \mathsf{F}d\boldsymbol{Z}] \\ &= (\mathsf{det}\mathsf{F})[d\boldsymbol{X}, d\boldsymbol{Y}, d\boldsymbol{Z}] \\ &= JdV, \end{aligned} \tag{2.23}$$

where J is Jacobian of the motion.

Definition 2.1.7. If a motion $\boldsymbol{\phi}$ is such that there is no change in volume, then the motion is said to be ***isochoric***. In that case

$$J(\boldsymbol{X}, t) = \mathsf{det}\mathsf{F}(\boldsymbol{X}, t) = 1, \quad \forall \boldsymbol{X} \in \mathcal{B}_r, t > 0.$$

2.1.5 Strain Tensor

Let us investigate now how material line elements are stretched or contracted during an arbitrary deformation $\boldsymbol{\phi}(\cdot, t)$. The deformation tensor (2.12) is the fundamental measure of deformation which plays a very important role in capturing this information. Assume that $\boldsymbol{M}$ and $\boldsymbol{m}$ are unit vectors along $d\boldsymbol{X}$ and $d\boldsymbol{x}$, respectively. Thus,

$$\begin{aligned}\boldsymbol{M} &= \frac{d\boldsymbol{X}}{\|d\boldsymbol{X}\|} \rightarrow d\boldsymbol{X} = \boldsymbol{M}\|d\boldsymbol{X}\|,\\ \boldsymbol{m} &= \frac{d\boldsymbol{x}}{\|d\boldsymbol{x}\|} \rightarrow d\boldsymbol{x} = \boldsymbol{m}\|d\boldsymbol{x}\|.\end{aligned}$$

By using these two relations in $d\boldsymbol{x} = \mathbf{F}d\boldsymbol{X}$, we find

$$\boldsymbol{m}\|d\boldsymbol{x}\| = \mathbf{F}\boldsymbol{M}\|d\boldsymbol{X}\|,$$

and thus,

$$\begin{aligned}\boldsymbol{m}\|d\boldsymbol{x}\| \cdot \boldsymbol{m}\|d\boldsymbol{x}\| &= \mathbf{F}\boldsymbol{M}\|d\boldsymbol{X}\| \cdot \mathbf{F}\boldsymbol{M}\|d\boldsymbol{X}\|\\ (\boldsymbol{m}\cdot\boldsymbol{m})\|d\boldsymbol{x}\|^2 &= (\mathbf{F}\boldsymbol{M}\cdot\mathbf{F}\boldsymbol{M})\|d\boldsymbol{X}\|^2.\end{aligned}$$

By rewriting the upper equation and putting all together we get the relation between the lengths of line elements

$$\|d\boldsymbol{x}\|^2 = (\boldsymbol{M}\cdot(\mathbf{F}^{\mathsf{T}}\mathbf{F})\boldsymbol{M})\|d\boldsymbol{X}\|^2 = (\boldsymbol{M}\cdot\mathbf{C}\boldsymbol{M})\|d\boldsymbol{X}\|^2.$$

Here we have to be careful with the $\mathbf{F}^{\mathsf{T}}$ which is in the relation with $\mathbf{F}$ in the next form

$$\mathbf{F}^{\mathsf{T}} = \mathbf{F}\circ\boldsymbol{\phi}^{-1} : \mathbb{T}_{\boldsymbol{x}}\mathcal{B}_t \rightarrow \mathbb{T}_{\boldsymbol{X}}\mathcal{B}_r.$$

Actually it maps between its dual tangent spaces $\mathbb{T}^*$, but this is of no importance for us here, and we will neglect this fact. In differential geometry the connecting maps between $\mathbb{T}$ and $\mathbb{T}^*$ are named the ***metric maps***.

Definition 2.1.8. The ***right Cauchy deformation tensor*** is defined as

$$\mathbf{C} := \mathbf{F}^{\mathsf{T}}\mathbf{F}, \quad \mathbf{C} : \mathbb{T}_{\boldsymbol{X}}\mathcal{B}_r \rightarrow \mathbb{T}_{\boldsymbol{X}}\mathcal{B}_r, \tag{2.24}$$

and its component representation assumes the form

$$\mathbf{C}_{ij} = \mathsf{C}_{ij}\boldsymbol{E}_i \otimes \boldsymbol{E}_j, \quad \mathsf{C}_{ij} = \mathsf{F}_{ki}\mathsf{F}_{kj}.$$

Note that $\mathbf{C}$ is a Lagrangian measure of deformation.

In a similar way as above, we can define new tensor.

Definition 2.1.9. The ***left Cauchy deformation tensor*** is defined as

$$\mathbf{B} := \mathbf{F}\mathbf{F}^{\mathsf{T}}, \quad \mathbf{B} : \mathbb{T}_{\boldsymbol{x}}\mathcal{B}_t \to \mathbb{T}_{\boldsymbol{x}}\mathcal{B}_t, \tag{2.25}$$

and its component representation assumes the form

$$\mathbf{B}_{ij} = \mathsf{B}_{ij}\boldsymbol{e}_i \otimes \boldsymbol{e}_j, \quad \mathsf{B}_{ij} = \mathsf{F}_{ik}\mathsf{F}_{jk}.$$

Note that this is an Eulerian measure of deformation.

Definition 2.1.10. The ***stretch*** in the direction $\boldsymbol{M}$ at $\boldsymbol{X}$ is defined as

$$\lambda(\boldsymbol{M}) = \frac{\|d\boldsymbol{x}\|}{\|d\boldsymbol{X}\|} = \sqrt{\boldsymbol{M} \cdot \mathbf{C}\boldsymbol{M}}. \tag{2.26}$$

Definition 2.1.11. The ***displacement*** $\boldsymbol{u}$ of a particle is defined as

$$\boldsymbol{u} := \boldsymbol{x} - \boldsymbol{X} = \boldsymbol{\phi}(\boldsymbol{X}, t) - \boldsymbol{X} = \boldsymbol{x} - \boldsymbol{\phi}^{-1}(\boldsymbol{x}, t). \tag{2.27}$$

Note that the displacement field can be regarded as either a Lagrangian field (independent variables: $\boldsymbol{X}$ and t) or an Eulerian field (independent variables: $\boldsymbol{x}$ and t). From (2.27) we get

$$\boldsymbol{x} = \boldsymbol{X} + \boldsymbol{u} \quad \to \quad \nabla|_{\boldsymbol{X}}\, \boldsymbol{x} = \nabla|_{\boldsymbol{X}}\, \boldsymbol{X} + \nabla|_{\boldsymbol{X}}\, \boldsymbol{u},$$

which can be written as

$$\mathbf{F} = \mathbf{I} + \nabla|_{\boldsymbol{X}}\, \boldsymbol{u}.$$

The ***displacement gradient*** is an important measure of deformation in the linearised theories of continuum mechanics.

2.1.6 The Spatial Gradient of Velocity

We now introduce kinematical variables that describe the instantaneous time rates of deformation. These variables, usually referred to as ***kinematical rate tensors***, are not in general the time rates of the deformation tensors introduced previously. The reason for this is that deformation tensors are functions of two configurations (a referential and a current configuration), whereas rate tensors are, by definition, functions of the current configuration alone. A fundamental rate tensor is the so-called ***velocity gradient tensor***.

Definition 2.1.12. The ***velocity gradient tensor*** $\mathbf{L}$ is defined as the spatial gradient of velocity, that is

$$\mathbf{L}(\boldsymbol{x}, t) := \nabla|_x \, \boldsymbol{v} \equiv \nabla \boldsymbol{v}(\boldsymbol{x}, t). \tag{2.28}$$

The component representation of this tensor is

$$\mathbf{L}_{ij} = \mathsf{L}_{ij} \boldsymbol{e}_i \otimes \boldsymbol{e}_j, \qquad \mathsf{L}_{ij} = \frac{\partial v_i}{\partial x_j}.$$

With the definition of the velocity gradient tensor we can find new interesting relation for the deformation gradient

$$\begin{aligned}
\dot{\mathbf{F}} &= \mathbf{L}\mathbf{F}, \\
\mathbf{L} &= \dot{\mathbf{F}}\mathbf{F}^{-1}, \\
\frac{dJ}{dt} = \dot{J} &= \frac{d}{dt}(\mathsf{det}\mathbf{F}) = (\mathsf{det}\mathbf{F})\mathsf{tr}(\dot{\mathbf{F}}\mathbf{F}^{-1}) = J\,\mathsf{tr}\mathbf{L} = J\,\nabla \cdot \boldsymbol{v}, \\
\dot{J} &= J\,\nabla \cdot \boldsymbol{v}.
\end{aligned}$$

Remark. For Isohoric motion $J = 1$, $\dot{J} = 0$ we see that divergence of the spatial velocity field equals to zero

$$\nabla \cdot \boldsymbol{v} = 0.$$

According to the observation made in Appendix A, any second-order tensor can be written as the sum of a symmetric and a skew-symmetric part. Thus, we can write

$$\mathbf{L} = \mathbf{D} + \mathbf{W},$$

where

$$\mathbf{D} := \frac{1}{2}(\mathbf{L} + \mathbf{L}^{\mathsf{T}}), \tag{2.29}$$

is the symmetric part of the velocity gradient, known as the ***stretching tensor*** or the ***strain-rate tensor***, and

$$\mathbf{W} := \frac{1}{2}(\mathbf{L} - \mathbf{L}^{\mathsf{T}}), \tag{2.30}$$

is its skew-symmetric part, usually called the ***spin tensor***.

2.2 Yield function

Quantitative treatment of the mechanics of a granular material can be traced back to Coulomb [Cou76], whose name is associated with a model of the material as an elastic-plastic continuum which yields by shearing on planes where shear stress τ first reaches a value related to the normal stress σ by

$$\tau = \sigma \tan \varphi + c, \tag{2.31}$$

where φ and c are parametres characteristic of material.

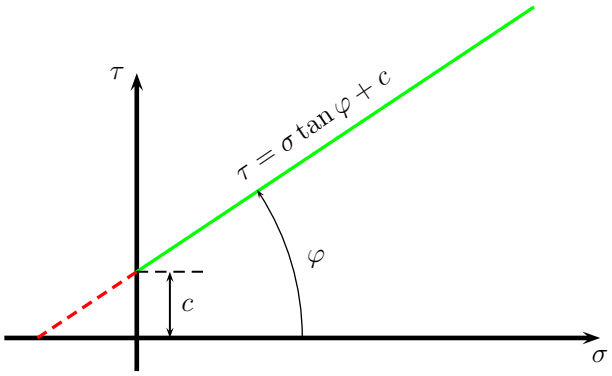

Figure 2.1: Coulomb yield criteria – friction law.

If c takes a non-vanishing positive value the material is said to be ***cohesive***. We shall be concerned with non-cohesive materials (typical sand, powder) for which the only material parameter is φ, called the ***angle of internal friction***. The law (2.31) is named as ***Coulomb yield criteria***.

2.2.1 Mohr Circle

To derive a connection between (2.31) and components of a stress tensor $\mathbf{T}$ we need first to explain the 2D stress analysis with a Mohr circle principle.

Each stress vector $\boldsymbol{t} = \mathbf{T}\boldsymbol{n}$, where $\boldsymbol{n}$ is a normal vector to the arbitrary surface, on the arbitrary surface trough the point $\boldsymbol{x}$, can be uniquely decomposed in two components: one in the direction of normal vector $\boldsymbol{n}$, which we will denote σ_n and is named ***normal component*** and other in the direction parallel to the surface which we will denote τ_n and is named ***tangent*** or ***shear component***. It follows

$$\boldsymbol{t} \cdot \boldsymbol{t} = \sigma_n^2 + \tau_n^2.$$

We see that components σ_n and τ_n are defined with stress tensor and normal vector.

By the spectral decomposition theorem (i.e. [Gur81]), each symmetric tensor can be rewritten in diagonal form. From the stress tensor we have

$$\mathbf{U}^{\mathsf{T}}\mathbf{T}\mathbf{U} =: \begin{pmatrix} \sigma_1 & 0 & 0 \\ 0 & \sigma_2 & 0 \\ 0 & 0 & \sigma_3 \end{pmatrix}, \qquad \sigma_1 \geq \sigma_2 \geq \sigma_3.$$

We will look for the case, when all principal values are not equal. Let us write the system of equations

$$\begin{aligned} n_1^2 + n_2^2 + n_3^2 &= 1, \\ \sigma_1 n_1^2 + \sigma_2 n_2^2 + \sigma_3 n_3^2 &= \sigma_n, \\ \sigma_1^2 n_1^2 + \sigma_2^2 n_2^2 + \sigma_3^2 n_3^2 &= \sigma_n^2 + \tau_n^2, \end{aligned}$$

which gives us the solution of the components for the normal surface vector

$$\begin{aligned} \left[\sigma_n - \frac{1}{2}(\sigma_2 + \sigma_3)\right]^2 + \tau_n^2 &= R_1^2, \\ \left[\sigma_n - \frac{1}{2}(\sigma_3 + \sigma_1)\right]^2 + \tau_n^2 &= R_2^2, \\ \left[\sigma_n - \frac{1}{2}(\sigma_1 + \sigma_2)\right]^2 + \tau_n^2 &= R_3^2, \end{aligned} \tag{2.32}$$

with

$$\begin{aligned} R_1^2 &:= \frac{1}{4}(\sigma_2+\sigma_3)^2 + (\sigma_1-\sigma_2)(\sigma_1-\sigma_3)n_1^2 - \sigma_2\sigma_3, \\ R_2^2 &:= \frac{1}{4}(\sigma_3+\sigma_1)^2 + (\sigma_1-\sigma_2)(\sigma_2-\sigma_3)n_2^2 - \sigma_3\sigma_1, \\ R_3^2 &:= \frac{1}{4}(\sigma_1+\sigma_2)^2 + (\sigma_1-\sigma_3)(\sigma_2-\sigma_3)n_3^2 - \sigma_1\sigma_2. \end{aligned} \tag{2.33}$$

For specific values of n_1, n_2, n_3 the equations (2.32) represents the circle in the σ_n, τ_n plane. Exactly, equations (2.32) represent circles on the unit sphere, defined with the values of n_1, n_2, n_3.

For the further studies we need a definitions of a Yield function and the Yield strength.

Definition 2.2.1 (Yield function, Yield strength)**.** The convex function $\mathcal{F} : \mathbb{T}_xB \times \mathbb{T}_xB \to \mathbb{R}$, where $\mathbb{T}_xB \times \mathbb{T}_xB$ is a space of rank-two tensor fields, determines the yield surface in the space of stress, i.e. the set of tensors $\mathbf{T}$ s.t.

$$\mathcal{F} = \mathcal{F}(\mathbf{T}). \tag{2.34}$$

Equation (2.34) is called a ***yield function***. The condition when the value of yield function is equal to 0,

$$\mathcal{F}(\mathbf{T}) = 0, \tag{2.35}$$

is called a ***yield strength***. The case of $\mathcal{F} > 0$ is forbidden, this is related to the Mohr-Coulomb criteria in the next subsection (point 3 in the placement of Coulomb yield function on the graph of Mohr circle). The yield strength defines a point where material model switches from i.e. rigid to plastic or elastic to plastic.

Material models for which

$$\mathcal{F}(\mathbf{T}) \leq 0,$$

are called ***rate independent plasticity models***. The term "rate independent" refers to the lack of an explicite time. Rate independent plasticity models provide just a limited class of initial value problems. Rate dependant plasticity models consider a wider space of problems, but the PDE's become more complicated.

2.2.2 Mohr - Coulomb Yield function

To model granular flow we need a relation between a shear stress and yield criteria - failure criteria. For the 2D case, there is a graphic approach to find this relation. If we plot Mohr circle and Coulomb yield function on the same plot (Fig. 2.2), the relation is immediately seen.

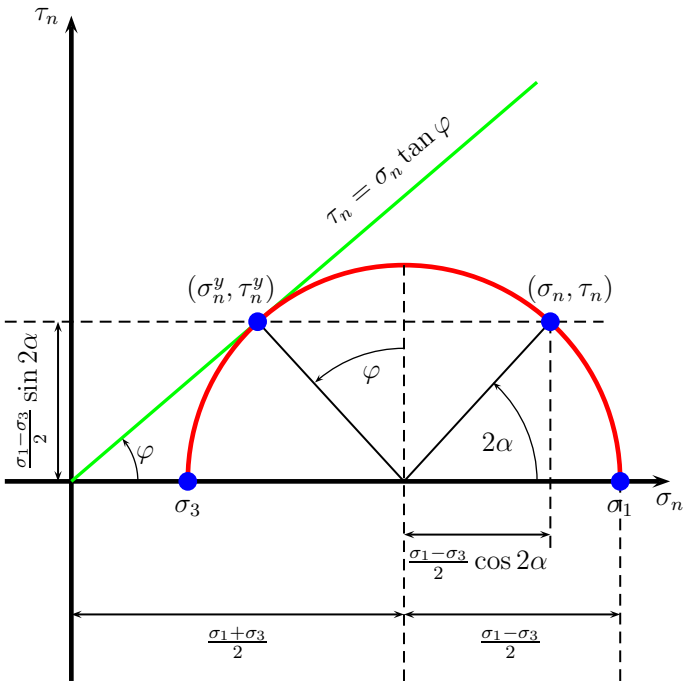

Figure 2.2: Mohr big circle + Coulomb yield criteria.

On the Fig. 2.2 α represent the angle between the normal surface vector and one of the principal stress direction. If n_1 changes then the components of stress vector change to. The aim is to find such a direction, which will satisfy the yield criteria.

Looking on Fig. 2.2 there exist three possibilities of placing Mohr circle with different radius:

(1) The Coulomb line can lie entirely above Mohr's circle. This is the case when

$$\tau_n < \sigma_n \tan\varphi,$$

and no slip condition will be satisfied. We say that material is in a state of stable static equilibrium.

(2) The Coulomb line may touch the Mohr's circle. This is the case of

$$\tau_n = \sigma_n \tan\varphi,$$

and slip condition is satisfied. Granular material will develop a slip and cause the start of flow.

(3) The Coulomb line cuts the circle. This is the case

$$\tau_n > \sigma_n \tan\varphi,$$

but this is the forbidden state in a Coulomb material.

If we write the values for stress vector components and the yield criteria

$$\begin{aligned}
\sigma_n &= \frac{\sigma_1 + \sigma_3}{2} + \frac{1}{2}(\sigma_1 - \sigma_3)\cos 2\alpha, \\
\tau_n &= \frac{1}{2}(\sigma_1 - \sigma_3)\sin 2\alpha, \\
\tau_n &= \sigma_n \tan\varphi, \\
\varphi &= 2\alpha,
\end{aligned}$$

we derive the relation of the yield criteria in the principal components of the stress tensor

$$\frac{\sigma_1}{\sigma_3} = \frac{1 + \sin\varphi}{1 - \sin\varphi}. \tag{2.36}$$

It is seen that this failure criterion is independent of the intermediate principal stress σ_2.

2.2.3 Conical or Extended Von Mises Yield function

As an alternative, we could use some other measure of the shear and normal stresses. One such possibility is to work in terms of the octahedral stresses ([Lub90]) defined by

$$\begin{aligned}
\sigma_{\text{oct}} &= \frac{1}{3}(\sigma_1 + \sigma_2 + \sigma_3) =: \langle\sigma\rangle, \\
\tau_{\text{oct}} &= \frac{1}{3}\sqrt{(\sigma_1 - \sigma_2)^2 + (\sigma_2 - \sigma_3)^2 + (\sigma_3 - \sigma_1)^2}.
\end{aligned}$$

The differences $(\sigma_1 - \sigma_2)^2$, $(\sigma_2 - \sigma_3)^2$, $(\sigma_3 - \sigma_1)^2$ are the diameters of the appropriate Mohr's circles, as can be seen from Fig. 2.2, this are equal to twice the greatest shear stress. Octahedral shear stress is proportional to the root mean square of the three maximum shear stresses. We can postulate a yield function in which τ_{oct} is proportional to σ_{oct}. The relation is

$$\tau_{\text{oct}} = \sqrt{\frac{2M}{3}}\sigma_{\text{oct}}, \tag{2.37}$$

where the constant of proportionality is used in such a way to have algebraic convenience in latter computations. If we express Mohr-Coulomb yield condition in the same fashion, we find that

$$M = \sin\varphi.$$

Thus we can write Conical yield condition as

$$(\sigma_1 - \sigma_2)^2 + (\sigma_2 - \sigma_3)^2 + (\sigma_3 - \sigma_1)^2 = 2\langle\sigma\rangle^2 \sin^2\varphi. \tag{2.38}$$

We confine ourself to the Conical yield function by setting

$$\mathcal{F}(\mathbf{T}) = (\sigma_1 - \sigma_2)^2 + (\sigma_2 - \sigma_3)^2 + (\sigma_3 - \sigma_1)^2 - 2\langle\sigma\rangle^2 \sin^2\varphi. \tag{2.39}$$

As we know each tensor can be decomposed in its spherical and deviatoric part (appendix A). For the stress tensor (written in diagonal form) we express it as

$$\mathbf{T} = \overset{\circ}{\mathbf{T}} + \overset{*}{\mathbf{T}} = \langle\sigma\rangle\mathbf{I} + \overset{*}{\mathbf{T}}.$$

The deviatoric part is expressed as

$$\overset{*}{\mathbf{T}} = \begin{pmatrix} \sigma_1 - \langle\sigma\rangle & 0 & 0 \\ 0 & \sigma_2 - \langle\sigma\rangle & 0 \\ 0 & 0 & \sigma_3 - \langle\sigma\rangle \end{pmatrix},$$

and its norm $\|\overset{*}{\mathbf{T}}\|^2$ equals to

$$\|\overset{*}{\mathbf{T}}\|^2 = (\sigma_1 - \langle\sigma\rangle)^2 + (\sigma_2 - \langle\sigma\rangle)^2 + (\sigma_3 - \langle\sigma\rangle)^2.$$

With a bit of algebra we can derive the next equality ([Ned92] chap.9)

$$\|\overset{*}{\mathbf{T}}\|^2 = (\sigma_1 - \sigma_2)^2 + (\sigma_2 - \sigma_3)^2 + (\sigma_3 - \sigma_1)^2,$$

and then we can write (2.39) in a more compact form

$$\mathcal{F}(\mathbf{T}) = \|\overset{*}{\mathbf{T}}\|^2 - k^2\langle\sigma\rangle^2, \qquad k^2 = 2\sin^2\varphi. \tag{2.40}$$

2.2.4 Pitman-Schaeffer Conical Yield function

Conical condition is used in modelling of isohoric type of motions, but the granular media is also compressible and the extension to consider the effects of compressibility was introduced in [PS87]. Modification is derived by the expansion in Taylor series around the critical state (incompressible situation) and truncated after the quadratic term. New form of a yield condition is

$$\mathcal{F}(\mathbf{T}) = \|\overset{*}{\mathbf{T}}\|^2 - k^2\left\{P(\rho)^2 - [P(\rho) - \langle\sigma\rangle]^2\right\}, \tag{2.41}$$

where is $P(\rho)$ related to the static pressure in the granular flow (if we relate it to the Newtonian fluids). As we can see in the critical state the static pressure equals the averaged stress and we obtain the incompressible variant of a yield condition. Among the first collected written work about the compressibility effects in granular (soil mechanics) are written in the work of [SW68]. They consider the dilation and consolidation yield loci.

2.3 Associated Flow Rule

The kinematics of yield condition, based on plasticity is first mentioned in the work of Drucker & Prager [DP52]. In this picture the strain-rate tensor and stress tensor at yield are related trough the plastic potential flow.

An ***associated flow rule*** relates the plastic strain-rate to the yield function. It is obtained from what is referred to as the ***maximum dissipation postulate*** ([Lub90]), which states that among all admissible values of stress, we ought to select those which maximises the plastic dissipation. In the rate independent case, plastic strain is varied over the yield surface $\mathcal{F}$, to find an extremum in the plastic dissipation. The extremum occurs when

$$\mathbf{D} = \lambda\nabla\mathcal{F}(\mathbf{T}) = \lambda\left(\frac{\partial\mathcal{F}}{\partial\sigma_1}, \frac{\partial\mathcal{F}}{\partial\sigma_2}, \frac{\partial\mathcal{F}}{\partial\sigma_3}\right), \tag{2.42}$$

where λ is a Lagrange multiplier which is determined from the constraint that $\mathbf{T}$ lies on the yield surface. The $\nabla\mathcal{F}(\mathbf{T})$ is the outward normal on a yield surface. This equation has the interpretation that the strain-rate is normal to the yield surface when the yield function is expressed in terms of stress. Trace of the strain-rate is always positive. Thus, deformation is always accompanied by dilation, and this arises naturally from the theory.

Remark. The associated flow rule applies when the yield function is smooth. If not, as is for example the case of Tresca, models for crystal plasticity, the strain-rate can be defined as a convex linear combination of the normals to the adjacent facets.

2.4 Constitutive relation

A constitutive material model, needed to complet the granular flow model is composed of a yield function $\mathcal{F}(\mathbf{T})$, and a rule for the direction of the strain-rate, such as the associated flow rule (2.42). For the compressible type of extended Conical yield function is

$$\mathcal{F}(\mathbf{T}) = \|\overset{*}{\mathbf{T}}\|^2 - 2\sin^2\varphi\left\{P(\rho)^2 - [P(\rho) - \langle\sigma\rangle]^2\right\}.$$

and expressed in terms of the stress tensor invariants reads

$$\mathcal{F}(\mathbf{T}) = \frac{2}{3}\,\mathrm{I}_{\mathbf{T}}^2 - 2\,\mathrm{II}_{\mathbf{T}} - 2\sin^2\varphi\left\{P(\rho)^2 - \left[P(\rho) - \frac{1}{3}\,\mathrm{I}_{\mathbf{T}}\right]^2\right\}.$$

Combining flow rule and yield condition we derive a constitutive relation for the granular flow for the incompressible flow

$$\mathbf{T} = P\mathbf{I} + \frac{P\sin\varphi}{\sqrt{\mathrm{II}_{\mathbf{D}}}}\mathbf{D} = P\mathbf{I} + \frac{P\sin\varphi}{\|\mathbf{D}\|}\mathbf{D} \tag{2.43}$$

and for the compressible type of flow

$$\begin{aligned}\mathbf{T} &= P(\rho)\mathbf{I} - \frac{P(\rho)f(\mathbf{D})}{2\sin^2\varphi}\,\mathrm{I}_{\mathbf{D}}\mathbf{I} + P(\rho)f(\mathbf{D})\overset{*}{\mathbf{D}},\\ f(\mathbf{D}) &= \frac{2\sin^2\varphi}{\sqrt{4\sin^2\varphi\,\mathrm{II}_{\mathbf{D}} + (1-\frac{4}{3})\sin^2\varphi\,\mathrm{I}_{\mathbf{D}}^2}}.\end{aligned} \tag{2.44}$$

The incompressible flow can be obtained from the compressible one by setting $\mathrm{I}_{\mathbf{D}} = 0$.

2.5 Closure Relation

Closure relation for the pressure in the case of compressible flows can have different form. It is not derived from some basic physical principles, but it is based on a bit intuitive picture. First we would need definition of the density and dilation (consolidation) of granular matter.

2.5.1 Density and Dilation of Granular Materials

In granular materials there are two densities of interest, the density of the particles themselves, which we will call the ***solid density*** and denote by ρ_s, and the density of the mixture of solid and the ***interstitial fluid*** (gas or liquid) which is known as the ***bulk density*** denoted by ρ_b. Provided the particles are not porous, the solid density can be measured by the usual techniques of liquid displacement and the bulk density can be obtained from the ratio of the mass and volume of a sample.

These two densities are related by

$$\rho_b := \rho_s(1 - \nu) + \rho_f \nu, \tag{2.45}$$

where ν is the ***void fraction*** defined as the volumetric fraction of the material occupied by the interstitial fluid and ρ_f is the density of interstitial fluid.

In a motion, deformation of granular flow is always accompanied by volume changes. We can explain it very easily. If an array of identical spherical grains at closest packing is subject to a load so as to cause a shear deformation, then from pure geometrical consideration particles must ride one over another it follows that an increase of the volume of the bulk will occur (see Fig. 2.3). This property was termed ***dilatancy*** by Reynolds in 1885. The opposite effect, when the volume is redused is termed ***consolidation***.

2.5.2 Pressure – Density relation

As we saw that the deformation of granular material is always accompanied by the volume change, this can not go over some limit densities. When we reach the

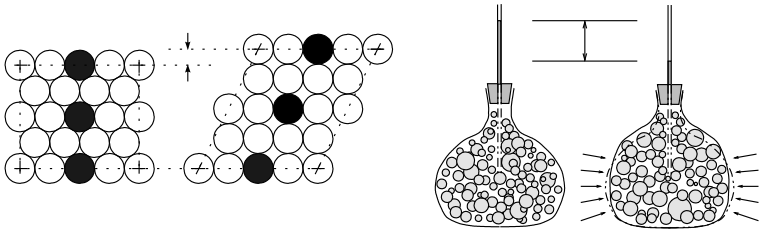

Figure 2.3: Explaining volume changes: (left) circular disks in closest packing being deformed in a pure shear way. (right) a rubber bellows filled with a granular material of a densest pack and sealed with a plug and pore space filled with water, of which filling is made visible with by the liquid level in a pipette. Outside pressure deforms the content also by shear, the water level in the pipette falls as a result of pore space extension. (Similar effect is the drying of a sand near by a feet, when walking on a sandy beach.) ([BP02])

state of closest packing then the pressure would rise to the infinity. The opposite situation is when the volume would increase till that limit, when the particles would start to loose permanent contacts with the neighboring grains, then the pressure would go to zero limit. This intuitive interpretation of a pressure, is given by different pressure-density relations. We will use two of them

(1)

$$P(\rho) = P_0 \left(\frac{\rho}{\rho_0}\right)^{1/\beta}, \qquad \beta \in [10^{-4}, 10^{-1}], \tag{2.46}$$

where

$$\rho_0 = \frac{\rho_{\max} + \rho_{\min}}{2}, \quad P_0 = \gamma \rho_0.$$

(2)

$$P(\rho) = \begin{cases} 0 & ; \quad \rho \leq \rho_{\min} \\ P_0 \frac{y(\rho)}{1-y(\rho)} & ; \quad \rho_{\min} < \rho < \rho_{\max} \\ \infty & ; \quad \rho \geq \rho_{\max} \end{cases} \tag{2.47}$$

where

$$y(\rho) = \frac{\rho - \rho_{\min}}{\rho_{\max} - \rho_{\min}}.$$

2.6 Balance Laws and Equations of Motion

2.6.1 Mass Conservation

In continuum mechanics, each body $\mathscr{B}$ possesses an unchanging property, called mass, which is a non-negative dimensional number, denoted by m or $m(\mathscr{B})$. We express the invariance of mass by

$$\frac{\mathrm{D}}{\mathrm{D}t} m(\mathscr{B}) = 0. \tag{2.48}$$

Above,

$$\frac{\mathrm{D}}{\mathrm{D}t}$$

represents the material time derivative, i.e. the derivative with respect to time, keeping $\boldsymbol{X}$ fixed; for a Lagrangian field this is simply the partial derivative with respect to time, whereas for Eulerian fields it involves a total derivative with respect to time. Mass is considered to be a primitive concept relying on special problems to provide interpretations of mass as well as methods for measuring it. It is commonly defined to be a measure of the amount of material contained in the body $\mathscr{B}$. The mass of a body is assumed to obey the following two intuitive properties:

(1)
$$m(\mathscr{P}_1 \cup \mathscr{P}_2) = m(\mathscr{P}_1) + m(\mathscr{P}_2),$$
for any two disjoint parts of $\mathscr{B}$, i.e. $\mathscr{P}_1$, $\mathscr{P}_2 \subset \mathscr{B}$ and $\mathscr{P}_1 \cap \mathscr{P}_2 = \emptyset$.

(2)
$$m(\mathscr{P}) \to 0 \ \text{ as } \ v(\mathscr{P}) \to 0,$$
where $v(\mathscr{P})$ denotes the volume of $\mathscr{P} \subset \mathscr{B}$.

In continuum mechanics we consider bodies whose mass is distributed ***continuously***. Thus, we need to be able to describe the mass of any portion of the body, however small it might be. This is achieved by postulating the existence of a mass density. Now, let us consider two families of "shrinking" sets in the reference and current configurations, with the following properties:

(1) in the ***reference configuration***:

$$\mathcal{P}_0^{(n)} \subset \mathcal{B}_r, \quad \mathcal{P}_0^{(n+1)} \subset \mathcal{P}_0^{(n)}, \quad \boldsymbol{X} \in \mathcal{P}_0^{(n)}, \quad \forall n \geq 0,$$

with $\mathcal{P}_0^{(n)} \to \{\boldsymbol{X}\}$, as $n \to \infty$, i.e. the sets $\mathcal{P}_0$ "shrink" to the point $\boldsymbol{X}$.

(2) in the ***current configuration***:

$$\mathcal{P}_t^{(n)} \subset \mathcal{B}_t, \quad \mathcal{P}_t^{(n+1)} \subset \mathcal{P}_t^{(n)}, \quad \boldsymbol{x} \in \mathcal{P}_t^{(n)}, \quad \forall n \geq 0,$$

Again, we require $\mathcal{P}_t^{(n)} \to \{\boldsymbol{x}\}$, as $n \to \infty$, with the same interpretation as above.

Definition 2.6.1 (Mass Density)**.**

(1) The reference mass density of $P \in \mathscr{B}$ is defined as

$$\rho_0(\boldsymbol{X}) := \lim_{n\to\infty} \frac{m(\mathcal{P}_0^{(n)})}{v(\mathcal{P}_0^{(n)})}$$

(2) The current mass density of the same point $P \in \mathscr{B}$ is by definition

$$\rho_t(\boldsymbol{x}) := \lim_{n\to\infty} \frac{m(\mathcal{P}_t^{(n)})}{v(\mathcal{P}_t^{(n)})}$$

Above $v(\mathcal{P})$ represents the volume of $\mathcal{P}$. The important point here is that the mass density depends on the configuration but the mass of any part of $\mathscr{B}$ is preserved during a given motion.

The ***global form*** of the principle of ***mass conservations*** is

$$\int_{\mathcal{P}_0} \rho_0(\boldsymbol{X}) dV \equiv \int_{\mathcal{P}_t} \rho_t(\boldsymbol{x}) dv, \quad \forall \mathcal{P}_0 \in \mathcal{B}_r, \quad \mathcal{P}_t = \boldsymbol{\phi}(\mathcal{P}_0, t). \tag{2.49}$$

This is a ***global*** (or ***integral***) principle, because it applies to arbitrary regions rather than to arbitrary points of the continuum body. We would like to have more precise information about what happens at individual points in the continuum, and that is achieved by using the so-called

Theorem 2.6.1 (Localisation Theorem)**.** *Let χ be a continuous scalar, vector, or tensor field defined on an open set $\mathcal{P}$ in the three-dimensional Euclidean space. Then, given any $\boldsymbol{x}_0 \in \mathcal{P}$,*

$$\chi(\boldsymbol{x}_0) = \lim_{\delta \to 0} \frac{1}{V(\Omega_\delta)} \int_{\Omega_\delta} \chi dV,$$

where Ω_δ $(\delta > 0)$ is the closed ball of radius δ centred at $\boldsymbol{x}_0$, and $V(\Omega_\delta)$ is the volume of Ω_δ.

Next important law is a ***local form*** of the principle of mass conservation in the Eulerian description. By writing (2.48) for the current configuration,

$$\frac{d}{dt} \int_{\mathcal{P}_t} \rho(\boldsymbol{x}, t) dv = 0,$$

taking into account the Transport Theorem, and then applying the Localisation Theorem, we find

$$\dot{\rho}(\boldsymbol{x}, t) + \rho(\boldsymbol{x}, t) \nabla \cdot \boldsymbol{v}(\boldsymbol{x}, t) = 0, \quad \forall \boldsymbol{x} \in \mathcal{B}_t, \ t > 0, \tag{2.50}$$

This is the differential form of (2.48), also known as the ***spatial equation of continuity***.

2.6.2 Momentum Conservation

Let $\mathcal{P}_t \subset \mathcal{B}_t$ be an arbitrary material region in the current configuration (material region = consisting of material points).

Definition 2.6.2. (1) The ***linear momentum***, $\boldsymbol{M}(\mathcal{P}_t)$, of the material occupying $\mathcal{P}_t$ in the current configuration is defined by

$$\boldsymbol{M}(\mathcal{P}_t) := \int_{\mathcal{P}_t} \rho(\boldsymbol{x}, t) \boldsymbol{v}(\boldsymbol{x}, t) dv. \tag{2.51}$$

(2) If $\boldsymbol{x} \in \mathcal{P}_t$ is the position vector of a representative point of $\mathcal{P}_t \subset \mathcal{B}_t$, relative to an origin $\boldsymbol{o}$, then the ***angular momentum*** of $\mathcal{P}_t$ with respect to $\boldsymbol{o}$ is defined by

$$\boldsymbol{H}(\mathcal{P}_t) := \int_{\mathcal{P}_t} \boldsymbol{x} \wedge (\rho(\boldsymbol{x}, t) \boldsymbol{v}(\boldsymbol{x}, t)) \, dv. \tag{2.52}$$

Definition 2.6.3. The ***resultant force*** acting on the material occupying $\mathcal{P}_t \subset \mathcal{B}_t$ in the current configuration is defined by

$$\boldsymbol{F}(\mathcal{P}_t) := \int_{\mathcal{P}_t} \rho \boldsymbol{b}\, dv + \int_{\partial\mathcal{P}_t} \boldsymbol{t}(\boldsymbol{n}) da, \tag{2.53}$$

where $\boldsymbol{b} = \boldsymbol{b}(\boldsymbol{x}, t)$ is the ***body force***; this latter quantity represents distributed force defined per unit mass in the current configuration due to an external agency, usually gravitation. In (2.53), $\boldsymbol{t}(\boldsymbol{n}) = \boldsymbol{t}(\boldsymbol{x}, t, \boldsymbol{n})$ represents the ***Cauchy traction (stress) vector*** (force measured per unit current surface area of $\partial\mathcal{P}_t$. The indicated dependence on $\boldsymbol{x}$ and the outward unit normal to $\partial\mathcal{P}_t$, $\boldsymbol{n}$, is intended to convey that $\boldsymbol{t}$ depends on the position but also on the orientation of the material surface upon which it acts. The interpretation of this force depends of the relative position of $\partial\mathcal{P}_t$:

(1) at points $\boldsymbol{x} \in \partial\mathcal{P}_t$ interior to $\mathcal{B}_t$, the stress vector $\boldsymbol{t}(\boldsymbol{x}, t, \boldsymbol{n})$ represents force per unit area exerted on $\mathcal{P}_t$ by the material outside this region.

(2) at points $\boldsymbol{x} \in \partial\mathcal{P}_t \cap \partial\mathcal{B}_t$ (i.e., on the surface of the body), the stress vector $\boldsymbol{t}(\boldsymbol{x}, t, \boldsymbol{n})$ represents force per unit area applied to the surface of the body by an external agency, and we shall refer to this as ***surface traction***.

Definition 2.6.4. The ***resultant torque*** with respect to $\boldsymbol{o}$ acting on the material occupying $\mathcal{P}_t \subset \mathcal{B}_t$ in the current configuration is defined by

$$\boldsymbol{G}(\mathcal{P}_t;\ \boldsymbol{o}) := \int_{\mathcal{P}_t} \boldsymbol{x} \wedge (\rho \boldsymbol{b})\, dv + \int_{\partial\mathcal{P}_t} \boldsymbol{x} \wedge \boldsymbol{t}(\boldsymbol{n})\, da. \tag{2.54}$$

Conservation laws for the linear and angular momentum in current configuration are

Conservation of Linear Momentum:

$$\frac{\mathrm{D}}{\mathrm{D}t}\boldsymbol{M}(\mathcal{P}_t) = \boldsymbol{F}(\mathcal{P}_t), \quad \forall \mathcal{P}_t \subset \mathcal{B}_t, \tag{2.55}$$

Conservation of Angular Momentum:

$$\frac{\mathrm{D}}{\mathrm{D}t}\boldsymbol{H}(\mathcal{P}_t, \boldsymbol{o}) = \boldsymbol{G}(\mathcal{P}_t, \boldsymbol{o}), \quad \forall \mathcal{P}_t \subset \mathcal{B}_t, \tag{2.56}$$

and these hold independently of the choice of origin (although $\boldsymbol{H}$ and $\boldsymbol{G}$ do depend on such a choice!). By taking into account (2.53) and (2.54), we arrive

at the ***global forms of balance of linear momentum, and balance of angular momentum***,

$$\begin{aligned}\frac{\mathrm{D}}{\mathrm{D}t}\boldsymbol{M}(\mathcal{P}_t) &= \int_{\mathcal{P}_t}\rho\boldsymbol{b}\,dv + \int_{\partial\mathcal{P}_t}\boldsymbol{t}(\boldsymbol{n})\,da,\\ \frac{\mathrm{D}}{\mathrm{D}t}\boldsymbol{H}(\mathcal{P}_t,\boldsymbol{o}) &= \int_{\mathcal{P}_t}\boldsymbol{x}\wedge(\rho\boldsymbol{b})\,dv + \int_{\partial\mathcal{P}_t}\boldsymbol{x}\wedge\boldsymbol{t}(\boldsymbol{n})\,da,\end{aligned} \tag{2.57}$$

The global form of these two conservation laws is not very useful for understanding what happens at particular points of the continuum body. Fortunately, we can invoke the Localisation Theorem and use to derive the local form of these principles. This is what we are going to do next.

Theorem 2.6.2 (Cauchy's Stress Theorem)**.** *There exists a unique second-order Eulerian tensor field* $\mathbf{T}(\boldsymbol{x},t)$ *with* $(\boldsymbol{x},t)\in\mathcal{B}_t\times\mathbb{R}^+$*, so that*

$$\boldsymbol{t}(\boldsymbol{x},t,\boldsymbol{n}) = \mathbf{T}(\boldsymbol{x},t)\boldsymbol{n}, \forall\boldsymbol{x}\in\mathcal{B}_t,\ t>0. \tag{2.58}$$

This important theorem simply states that the stress vector $\boldsymbol{t}(\boldsymbol{n})$ depends linearly on the outward unit normal, $\boldsymbol{n}$. A more detailed discussion of this theorem and its implications can be seen in [TT65], [MH92] or [Gur81].

On substitution of $\boldsymbol{t}(\boldsymbol{x},t,\boldsymbol{n}) = \mathbf{T}(\boldsymbol{x},t)\boldsymbol{n}$ in (2.57), we obtain

$$\int_{\partial\mathcal{P}_t}\mathbf{T}(\boldsymbol{x},t)\boldsymbol{n}\,da = \int_{\mathcal{P}_t}\nabla\cdot\mathbf{T}(\boldsymbol{x},t)\,dv$$

by the ***Divergence Theorem***. Thus the Localisation Theorem helps us to deduce that

$$\frac{\mathrm{D}(\rho\boldsymbol{v})}{\mathrm{D}t} = \nabla\cdot\mathbf{T}+\rho\boldsymbol{b}. \tag{2.59}$$

This is the ***local form of the principle of balance of linear momentum***, also known as Cauchy's first equation of motion. If we assume the next relation ([MH92])

$$\frac{\mathrm{D}}{\mathrm{D}t}\int_{\mathcal{P}_t}\rho\boldsymbol{v}\,dv = \int_{\mathcal{P}_t}\rho\dot{\boldsymbol{v}}\,dv,$$

we can write the equation of motion as

$$\rho\dot{\boldsymbol{v}} = \nabla \cdot \mathbf{T} + \rho\boldsymbol{b}.$$

With the help of conservation of angular momentum, we can proof ([MH92]) that stress tensor is symmetric tensor

$$\mathbf{T} = \mathbf{T}^{\mathsf{T}}.$$

Now we can summarise system of equations, which will be used in the next chapter.

- ***equation of mass conservation***:

$$\dot{\rho} + \rho\nabla \cdot \boldsymbol{v} = 0,$$

- ***equation of motion*** (Cauchy's first equation of motion):

$$\rho\dot{\boldsymbol{v}} = \nabla \cdot \mathbf{T} + \rho\boldsymbol{b},$$

- ***equation of angular momentum balance*** (Cauchy's second equation of motion):

$$\mathbf{T} = \mathbf{T}^{\mathsf{T}}.$$

- ***constitutive relation***:

$$\mathbf{T} = P(\rho)\left[\left(1 - \frac{f(\mathbf{D})}{2\sin^2\varphi}\,\mathrm{I}_{\mathbf{D}}\right)\mathbf{I} + f(\mathbf{D})\,\overset{*}{\mathbf{D}}\right],$$

$$f(\mathbf{D}) = \frac{2\sin^2\varphi}{\sqrt{4\sin^2\varphi\,\mathrm{II}_{\mathbf{D}} + (1-\frac{4}{3})\sin^2\varphi\,\mathrm{I}_{\mathbf{D}}^2}},$$

$$\mathbf{D} = -\frac{1}{2}\left(\boldsymbol{\nabla}\boldsymbol{v} + \boldsymbol{\nabla}\boldsymbol{v}^{\mathsf{T}}\right),$$

  where we need also the closure relation $P = P(\rho)$, which will be defined in the next chapters.

Part I – Analysis

Chapter 3

1D Flow Equations

In this chapter we will derive one dimensional model for the compressible and incompressible granular flow. We will show that the system of compressible flow is hyperbolic. The incompressible case gives a trivial solution.

3.1 Model derivation

Full three dimensional system include coordinates $\{x, y, z, t\}$, the reduced one dimensional system reduces to the coordinates $\{x, t\}$. The dependant quantities are density and velocity

$$\rho = \rho(x, t),$$
$$v = v(x, t).$$

Further, we reduce the operators of a scalar function u, of the gradient

$$\nabla u = \frac{\partial u}{\partial x},$$

and divergence

$$\nabla \cdot u = \frac{\partial u}{\partial x}.$$

3.1.1 Equations of Motion

Complete reduction of 3D conservation laws of mass, linear momentum and constitutive relations to 1D is done with the use of upper simplifications of gradient and divergence

- **Mass conservation**:

$$\dot{\rho} + \rho \nabla \cdot \boldsymbol{v} = 0,$$

is reduced in the 1D form

$$\frac{\partial \rho}{\partial t} + v \frac{\partial \rho}{\partial x} + \rho \frac{\partial v}{\partial x} = 0.$$

- **Linear momentum conservation**:

$$\rho \dot{\boldsymbol{v}} = \nabla \cdot \mathbf{T} + \rho \boldsymbol{b},$$

is reduced in the 1D form

$$\frac{\partial v}{\partial t} + v \frac{\partial v}{\partial x} = \frac{\partial \mathsf{T}}{\partial x} + f.$$

- **Constitutive relation**:

the compressible 3D c.r. is

$$\mathbf{T} = P(\rho) \left[\left(1 - \frac{f(\mathbf{D})}{2 \sin^2 \varphi} \, \mathrm{I}_{\mathbf{D}} \right) \mathbf{I} + f(\mathbf{D}) \overset{*}{\mathbf{D}} \right],$$

$$f(\mathbf{D}) = \frac{2 \sin^2 \varphi}{\sqrt{4 \sin^2 \varphi \, \mathrm{II}_{\mathbf{D}} + (1 - \frac{4}{3}) \sin^2 \varphi \, \mathrm{I}_{\mathbf{D}}^2}},$$

and the incompressible 3D c.r. is

$$\mathbf{T} = P \left[\mathbf{I} + \frac{\sin \varphi}{\|\mathbf{D}\|} \mathbf{D} \right].$$

The reduced 1D form for the compressible c.r. is

$$\mathsf{T} = \left(1 - \frac{1}{\sqrt{a_1}} + \frac{4 a_2}{3 \sqrt{a_1}} \right) P(\rho) = \alpha_c \, P(\rho),$$

and the incompressible c.r. is

$$\mathsf{T} = \left(\sqrt{2} \sin^2 \phi + 1 \right) P = \alpha_{ic} \, P,$$

where are constants a_1 and a_2 defined as

$$a_1 := 1 + \frac{4}{3}\sin^2\phi,$$
$$a_2 := \sin^2\phi.$$

Now we need to transform all equations in the dimension less form. Let us introduce next transformations

$$x \to Lx,$$
$$t \to Tt,$$
$$v \to \frac{L}{T}v,$$
$$\rho \to \rho\,\rho_{\max},$$
$$P \to P\,\gamma\rho_{\max},$$

which gives 1D equations in the non-dimensional form used in the following section.

3.2 Analysis of the Model

In this section we will show the solutions of the one dimensional models derived in the previous section.

3.2.1 Incompressible Flow

When using upper dimensionless transformation on incompressible set of equation we obtain the next system

$$\begin{aligned} \frac{\partial v}{\partial x} &= 0, \\ \frac{\partial v}{\partial t} + v\frac{\partial v}{\partial x} &= \alpha_{ic}\frac{\partial \gamma\rho_{\max}}{\partial x} = 0. \end{aligned} \tag{3.1}$$

Collecting all together we get

$$\rho(x,t) = const., \qquad \frac{\partial v}{\partial x} = \frac{\partial v}{\partial t} = 0 \to v(x,t) = const.$$

This is a solution of the rigid body motion. As we can see, the 1D approximation for the incompressible type of granular flow produce very uniteresting case of granular rigid wire.

3.2.2 Compressible Flow

We shall do the same dimensionless procedure over the compressible equations of motion. Final system of equations read as

$$\begin{aligned} \frac{\partial \rho}{\partial t} + \frac{\partial}{\partial x}(\rho v) &= 0, \\ \frac{\partial v}{\partial t} + \frac{\partial}{\partial x}\left(\frac{1}{2}v^2\right) &= \alpha_c \gamma \rho_{\max}(1-k)\frac{\frac{\partial \rho}{\partial x}}{1-\rho}, \\ k &= \frac{\rho_{\min}}{\rho_{\max}}. \end{aligned} \tag{3.2}$$

Let us define the vector

$$\boldsymbol{q} := \begin{pmatrix} \rho \\ v \end{pmatrix},$$

and constant $\beta = \alpha_c \gamma \rho_{\max}(1-k) > 0$. We can rewrite the system in the quasi-linear form as

$$\frac{\partial \boldsymbol{q}}{\partial t} + \mathbf{A}\frac{\partial \boldsymbol{q}}{\partial x} = \mathbf{0}, \quad \text{where} \quad \mathbf{A} = \begin{pmatrix} v & \rho \\ \frac{\beta}{1-\rho} & v \end{pmatrix}.$$

The eigenvalues of the matrix $\mathbf{A}$ are

$$\lambda_{1,2} = v \pm \sqrt{\frac{\beta\rho}{1-\rho}} \in \mathbb{R}.$$

By the criteria ([Kev00]) of the type of eigenvalues of the matrix $\mathbf{A}$ we conclude that the system of 1D compressible type of granular flow is ***hyperbolic***. Velocities of granular waves depend on the friction constant and density. It is seen that it can have the same or different direction depending on the value of

$$\sqrt{\frac{\beta\rho}{1-\rho}}.$$

Chapter 4

2D Flow Equations

The following chapter will discuss the derivation and analysis of the 2D model of the SDGF equations of motion. We can imagine the experiment with Stokes geometry filled with dense granular fluid. Dependant variables are homogeneous of the degree 0 in the x direction, meaning $f(\alpha x) = f(x) = const.$ All the variations occur just in the y direction and the time t.

4.1 Model Derivation

As in the previous chapter, we need to reduce the full 3D equations to the 2D form. All vector dependant variables as velocity $\boldsymbol{v}$ remain with all its components, but components do vary just in coordinates (y, t). The geometry is as in a simple shear experiment. We have fixed boundary at $y = 0$ extending from $-\infty$ to ∞ and the forcing is set at the upper boundary $y = h$ with constant velocity (see Fig. 4.1).

We have dependant variables velocity $\boldsymbol{v}(y,t) = \{u(y,t), v(y,t)\}$, density $\rho = \rho(y,t)$ and pressure $p = p(y,t)$. First let us write the divergence of the stress tensor $\mathbf{T}$. If we plug the relations for velocity and pressure in the Eq. (2.44) and remembering that we have spatial derivatives just with respect to y, we derive the components of the stress divergence as

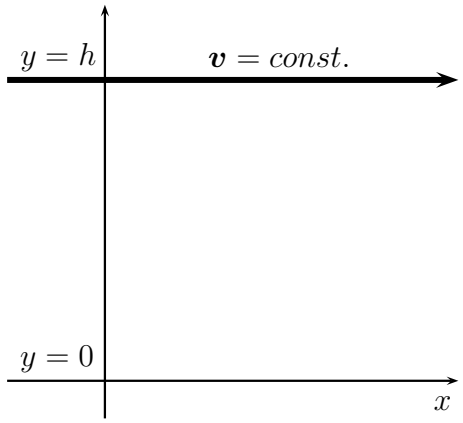

Figure 4.1: Figure explains the geometry for the 2D experiment of the SDGF equations. Boundary at $y = 0$ is fixed, and the boundary at $y = h$ has constant velocity, $x \in [-\infty, \infty]$.

$$
\begin{aligned}
(\nabla \cdot \mathbf{T})_x =& a_1 \frac{\frac{\partial p}{\partial y}\frac{\partial u}{\partial y} + p\frac{\partial^2 u}{\partial y^2}}{\sqrt{a_1\left(\frac{\partial u}{\partial y}\right)^2 + a_2\left(\frac{\partial v}{\partial y}\right)^2}} \\
& - a_1 \frac{p\,\frac{\partial u}{\partial y}\left(2a_1\frac{\partial u}{\partial y}\frac{\partial^2 u}{\partial y^2} + a_2\frac{\partial v}{\partial y}\frac{\partial^2 v}{\partial y^2}\right)}{\left(a_1\left(\frac{\partial u}{\partial y}\right)^2 + a_2\left(\frac{\partial v}{\partial y}\right)^2\right)^{3/2}}, \\
(\nabla \cdot \mathbf{T})_y =& \frac{\partial p}{\partial y} + (a_1 - 1)\frac{\frac{\partial p}{\partial y}\frac{\partial v}{\partial y} + p\,\frac{\partial^2 v}{\partial y^2}}{\sqrt{a_1\left(\frac{\partial u}{\partial y}\right)^2 + a_2\left(\frac{\partial v}{\partial y}\right)^2}} \\
& + (1 - a_1)\frac{p\,\frac{\partial v}{\partial y}\left(2a_1\frac{\partial u}{\partial y}\frac{\partial^2 u}{\partial y^2} + a_2\frac{\partial v}{\partial y}\frac{\partial^2 v}{\partial y^2}\right)}{\left(a_1\left(\frac{\partial u}{\partial y}\right)^2 + a_2\left(\frac{\partial v}{\partial y}\right)^2\right)^{3/2}},
\end{aligned}
\tag{4.1}
$$

where constants a_1 and a_2 are defined as

$$
\begin{aligned}
a_1 :=& \sin^2\varphi, \\
a_2 :=& 1 - \frac{4}{3}\sin^2\varphi.
\end{aligned}
$$

Then equations of motion in 2D are

$$\begin{aligned}\frac{\partial \rho}{\partial t}+\rho\frac{\partial v}{\partial y}+v\frac{\partial \rho}{\partial y}=&0,\\ \frac{\partial u}{\partial t}+v\frac{\partial u}{\partial y}=&\frac{1}{\rho}(\nabla\cdot\mathbf{T})_x+f_x,\\ \frac{\partial v}{\partial t}+v\frac{\partial v}{\partial y}=&\frac{1}{\rho}(\nabla\cdot\mathbf{T})_y+f_y.\end{aligned}\tag{4.2}$$

Next we transform the upper system in dimension less form. Moreover, we will assume that velocities in the y direction are much smaller than the velocities in x direction. This will lead to the introduction of the small parameter ε in the second velocity component v. Let us introduce the following transformations

$$\begin{aligned}y\rightarrow&Ly,\\ t\rightarrow&Tt,\\ u\rightarrow&\frac{L}{T}u,\\ v\rightarrow&\varepsilon\frac{L}{T}v,\\ \rho\rightarrow&\rho_{\max}\rho,\\ p\rightarrow&\rho_{\max}\frac{L^2}{T^2}\,p.\end{aligned}\tag{4.3}$$

Now, equations of motion have the same form, except the parameter ε will come into the play. Combining Eq. (4.1), Eq. (4.2) and Eq. (4.3) we obtain the following system

$$\begin{aligned}\frac{\partial \rho}{\partial t}+\varepsilon\left(\rho\frac{\partial v}{\partial y}+v\frac{\partial \rho}{\partial y}\right)=&0,\\ \frac{\partial u}{\partial t}+\varepsilon v\frac{\partial u}{\partial y}=&\frac{1}{\rho}h_x+f_x,\\ \varepsilon\frac{\partial v}{\partial t}+\varepsilon^2 v\frac{\partial v}{\partial y}=&\frac{1}{\rho}h_y+f_y,\end{aligned}\tag{4.4}$$

where h_x and h_y are functions defined as

$$h_x := a_1 \frac{\frac{\partial p}{\partial y}\frac{\partial u}{\partial y} + p\frac{\partial^2 u}{\partial y^2}}{\sqrt{a_1\left(\frac{\partial u}{\partial y}\right)^2 + \varepsilon^2 a_2\left(\frac{\partial v}{\partial y}\right)^2}} - a_1 \frac{p\,\frac{\partial u}{\partial y}\left(2a_1\frac{\partial u}{\partial y}\frac{\partial^2 u}{\partial y^2} + \varepsilon^2 a_2\frac{\partial v}{\partial y}\frac{\partial^2 v}{\partial y^2}\right)}{\left(a_1\left(\frac{\partial u}{\partial y}\right)^2 + \varepsilon^2 a_2\left(\frac{\partial v}{\partial y}\right)^2\right)^{3/2}},$$

$$h_y := \frac{\partial p}{\partial y} + (a_1 - 1)\frac{\frac{\partial p}{\partial y}\frac{\partial v}{\partial y} + \varepsilon p\,\frac{\partial^2 v}{\partial y^2}}{\sqrt{a_1\left(\frac{\partial u}{\partial y}\right)^2 + \varepsilon^2 a_2\left(\frac{\partial v}{\partial y}\right)^2}} + \varepsilon(1 - a_1)\frac{p\,\frac{\partial v}{\partial y}\left(2a_1\frac{\partial u}{\partial y}\frac{\partial^2 u}{\partial y^2} + \varepsilon^2 a_2\frac{\partial v}{\partial y}\frac{\partial^2 v}{\partial y^2}\right)}{\left(a_1\left(\frac{\partial u}{\partial y}\right)^2 + \varepsilon^2 a_2\left(\frac{\partial v}{\partial y}\right)^2\right)^{3/2}}.$$

In the following we deal with the upper set of equations (4.4), which will give us the prototype equation for the evolution of the SDGF motion. Introduction of the small parameter, calls for an asymptotic analysis, what will be the case.

4.2 Analysis of the Model

The 2D model (4.4) of SDGF was derived on the assumption of small velocities in the y direction compared to the one in the x direction. By this, we have introduced small parameter in the set of equations. The next step in the analysis of the system (4.4) will be to expand all the dependant variables in the regular asymptotic series

$$u(\boldsymbol{x}) := u_0(\boldsymbol{x}) + \varepsilon u_1(\boldsymbol{x}) + \varepsilon^2 u_2(\boldsymbol{x}) + \cdots + \varepsilon^n u_n(\boldsymbol{x}) + \mathcal{O}(\varepsilon^{n+1}).$$

In this contents let us define the expansions for dependant variables

$$\begin{aligned} u(\boldsymbol{x}) &:= u_0(\boldsymbol{x}) + \varepsilon u_1(\boldsymbol{x}) + \cdots && \text{velocity in } x \text{ direction},\\ v(\boldsymbol{x}) &:= v_0(\boldsymbol{x}) + \varepsilon v_1(\boldsymbol{x}) + \cdots && \text{velocity in } y \text{ direction},\\ p(\boldsymbol{x}) &:= p_0(\boldsymbol{x}) + \varepsilon p_1(\boldsymbol{x}) + \cdots && \text{pressure},\\ \rho(\boldsymbol{x}) &:= \rho_0(\boldsymbol{x}) + \varepsilon \rho_1(\boldsymbol{x}) + \cdots && \text{density}, \end{aligned} \tag{4.5}$$

where we have defined the indepentant variables as a vector $\boldsymbol{x} = (y, t)$.

To make the derivation more transparent, we preform the Taylor expansion of the functions h_x and h_y and retain the zero-th order terms. We get the following result

$$\begin{aligned} h_x =& \sqrt{a_1}\frac{\partial p}{\partial y} - \sqrt{a_1}p\frac{\frac{\partial^2 u}{\partial y^2}}{\frac{\partial u}{\partial y}} + \mathcal{O}(\varepsilon^2), \\ h_y =& \frac{\partial p}{\partial y} + \frac{a_1 - 1}{\sqrt{a_1}}\frac{\frac{\partial p}{\partial y}\frac{\partial v}{\partial y}}{\frac{\partial u}{\partial y}} + \mathcal{O}(\varepsilon^1). \end{aligned} \tag{4.6}$$

Inserting the (4.6) and (4.5) in the (4.4) we get a set of equations for different orders of ε. The zero-th order system read as

$$\frac{\partial \rho_0}{\partial t} = 0, \tag{4.7a}$$

$$\frac{\partial u_0}{\partial t} = \frac{\sqrt{a_1}}{\rho_0}\left(\frac{\partial p_0}{\partial y} - p_0\frac{\frac{\partial^2 u_0}{\partial y^2}}{\frac{\partial u_0}{\partial y}}\right), \tag{4.7b}$$

$$0 = \frac{1}{\rho_0}\frac{\partial p_0}{\partial y}\left(1 + \frac{a_1 - 1}{\sqrt{a_1}}\frac{\frac{\partial v_0}{\partial y}}{\frac{\partial u_0}{\partial y}}\right). \tag{4.7c}$$

From (4.7a) we conclude that

$$\rho_0 = \rho_0(y),$$

and from (4.7c), we have to consider two options:

(1)
$$\frac{\partial p_0}{\partial y} = 0 \rightarrow p_0 = p_0(t),$$

shows that pressure is only a function of time t. By the closure relations density and pressure are related and it follows that density is also only a function of time t, $\rho_0 = \rho_0(t)$. But using the property (4.7a) we can conclude that density and pressure are not functions of y neither of t, but are constants

$$\rho_0 = const., \quad p_0 = const.$$

(2)
$$1 + \frac{a_1 - 1}{\sqrt{a_1}}\frac{\frac{\partial v_0}{\partial y}}{\frac{\partial u_0}{\partial y}} = 0,$$

the second choice shows that velocity components are in relation

$$v_0(y,t) = \frac{\sqrt{a_1}}{1-a_1} u_0(y,t) + f(t). \tag{4.8}$$

The upper information on density and pressure combined with the equation (4.7b), lead us to the derivation of the final form for the velocity u_0

$$\frac{\partial u_0}{\partial t} = -\lambda \frac{\frac{\partial^2 u_0}{\partial y^2}}{\frac{\partial u_0}{\partial y}}, \quad \lambda = \sin\varphi \frac{p_0}{\rho_0} > 0. \tag{4.9}$$

Droping the index 0 and rewriting it in the new form we derive prototype backward nonlinear parabolic equation

$$\frac{\partial u}{\partial t} = -\lambda \frac{\partial}{\partial y}\left(\ln \frac{\partial u}{\partial y}\right). \tag{4.10}$$

The coefficient λ has values around the unity for the normal granular flow conditions ($\varphi = 30°$, $p_0 = 1-4$, $\rho_0 = 0.5-0.8$).

Stationary solution of the Eq. (4.10) is a linear function

$$u(y) = ky + n.$$

Is not the case that we obtained the same stationary solution as was derived in [Sch92] for the antiplane shear model

$$u(x,y) = a_1 x + a_2 y.$$

Equation (4.10) can be rewritten in more familiar form. We take the derivative with respect to y and introduce new variable

$$s = \frac{\partial u}{\partial y},$$

which is recognised as the shear stress. Then the Eq. (4.10) takes new form

$$\boxed{\frac{\partial s}{\partial t} = -\lambda \frac{\partial^2}{\partial y^2}(\ln s)} \tag{4.11}$$

We obtained the law for the shear stress evolution. Now raises the question, "Can we solve such PDE and what properties does it has?". We will try to answer that in the following subsections.

4.2.1 Separation of variables

We can obtain special solution of Eq. (4.10) with a separation of variables. If we write solution of (4.10) as

$$u(y,t) = Y(y)T(t),$$

and we plug it into the (4.10) we get

$$\frac{\partial T}{\partial t} = -\frac{\lambda}{Y}\frac{\partial}{\partial y}\left(\ln\frac{\partial Y}{\partial y}\right) = \alpha. \tag{4.12}$$

For $T(t)$ answer is trivial

$$T(t) = \alpha t + c_1,$$

but for the space variable $Y(y)$ we obtain second order ODE

$$Y'' + \frac{\alpha}{\lambda}Y'Y = 0,$$

with solution

$$Y(y) = \sqrt{\frac{2\lambda c_2}{\alpha}}\tanh\left(\sqrt{\frac{\alpha c_2}{2\lambda}}(y + c_3)\right).$$

Combining all together we obtain a special solution to the (4.10), which is

$$u(y,t) = \sqrt{\frac{2\lambda c_2}{\alpha}}(\alpha t + c_1)\tanh\left(\sqrt{\frac{\alpha c_2}{2\lambda}}(y + c_3)\right). \tag{4.13}$$

We observe that just special boundary conditions will satisfy (4.13), but in a realty such time dependant boundary conditions are very rare.

4.2.2 Discrete approximation

In this subsection we will follow analysis done in [WSS01]. In the work of [WSS01], they investigate the role of discretisation on the similar equation to the Eq. (4.10).

We study the numerical approximation of perturbation of (4.10) to the stationary state, i.e.

$$u(y,t) = ay + w(y,t). \tag{4.14}$$

On substitution of Eq. (4.14) into Eq. (4.10) we obtain

$$\frac{\partial w}{\partial t} = \frac{\partial}{\partial y}\left(F(w_y)\right), \quad \text{where} \quad F(w_y) = -\lambda \ln\left(a + \frac{\partial w}{\partial y}\right). \tag{4.15}$$

The semi-discrete (continuous-time/discrete-space) approximation of (4.15) is written as

$$\frac{\partial w_n}{\partial t} = \frac{1}{\Delta y}\left[F\left(\frac{w_{n+1} - w_n}{\Delta y}\right) - F\left(\frac{w_n - w_{n-1}}{\Delta y}\right)\right], \tag{4.16}$$

where $n = 1, \cdots, N-1$ and with the boundary conditions

$$w_0 = 0, \quad w_N = 0. \tag{4.17}$$

We write arguments of $F(\cdot)$ in Eq. (4.16) as

$$w'_{n+1/2} = \frac{w_{n+1} - w_n}{\Delta y}. \tag{4.18}$$

This is second order accurate centred finite difference approximation of spatial derivative, i.e.

$$w'_{n+1/2}(t) = w_y((n+1/2)\Delta x, t) + \mathcal{O}(\Delta x^2).$$

In the spirit of work [WSS01], we know that the discrete version of Eq. (4.15) is well-posed, with global solution. We can solve Eq. (4.16) numerically. We used the implicit midpoint method, written in general form as

$$\frac{w_n^{m+1} - w_n^m}{\Delta t} = \mathcal{F}\left(\frac{w^{m+1} + w^m}{2}\right), \tag{4.19}$$

where $w_n^m \approx w_n(t^m)$ and $t^m = m\Delta t$.

We have to solve next system of nonlinear equations

$$\begin{aligned}\frac{w_n^{m+1} - w_n^m}{\Delta t} = \frac{1}{\Delta y}\Bigg[&F\left(\frac{w_{n+1}^{m+1} + w_{n+1}^m - (w_n^{m+1} + w_n^m)}{2\Delta y}\right) \\ &-F\left(\frac{w_n^{m+1} + w_n^m - (w_{n-1}^{m+1} + w_{n-1}^m)}{2\Delta y}\right)\Bigg],\end{aligned} \tag{4.20}$$

where F is defined in (4.15).

In the Fig. 4.2 we show numerical results for the system (4.20). We used function

$$F(s) = -\lambda \ln(a + s),$$

with constants $\lambda = 1.0$ and $a = 0.1$. The space discretisation used $N = 100$ points on interval $y \in [0, 1]$, $\Delta y = 0.01$. Time interval was fixed $\Delta t = 10^{-4}$, and the initial data were

$$w(y) = 10^{-2} \sin(\pi\, x).$$

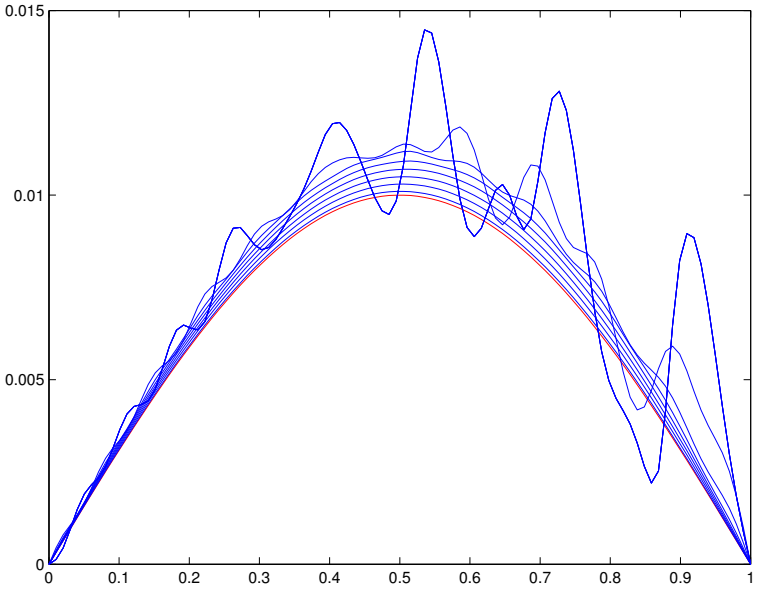

Figure 4.2: Figure show numerical result of Eq. (4.20). We used Dogleg method to solve nonlinear system of equations.

We observe, that the initial profile starts to grow and tries to develop δ peak, but after certain number of iteration we get oscillation. We see that our diffusion coefficient produce unstable results compared to one in the [WSS01]. If we write the equation (4.11) in the form

$$\frac{\partial s}{\partial t} = \frac{\partial}{\partial y}\left(D(s)\frac{\partial s}{\partial y}\right),$$

we get for diffusion coefficient

$$D(s) = -\frac{\lambda}{s}.$$

We know that $s \geq 0$ and then the diffusion coefficient is always negative, compared to the one in [WSS01]

$$D(s) = -\frac{\sin\alpha \sin\phi}{(1 + 2s\cos\phi + s^2)^{3/2}}(s - s_{\max}), \tag{4.21}$$

which has the interval where it is positive and interval where it is negative

$$D(s \leq s_{\max}) \geq 0, \quad D(s > s_{\max}) < 0.$$

In the Fig. 4.3 we see the numerical results for the diffusion coefficient (4.21). There is typical step advancing solution. At the end many steps will colaps into single one, resulting in the two single block movement.

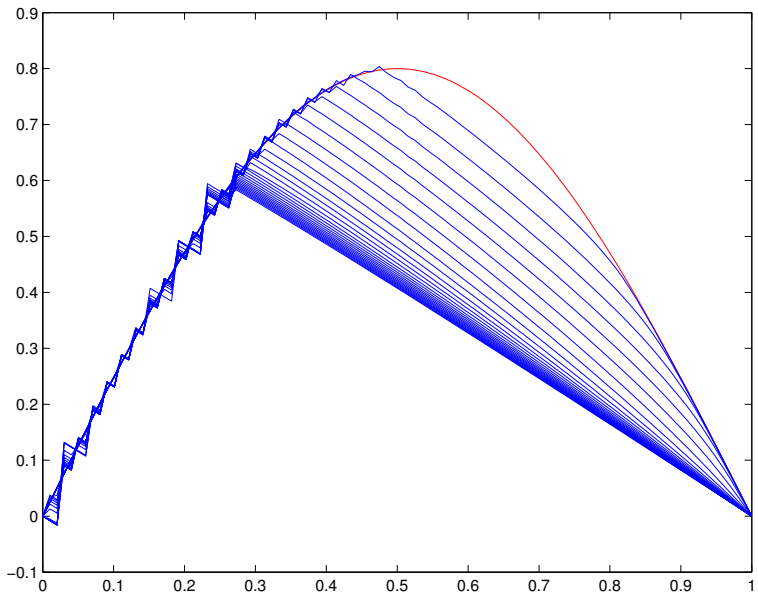

Figure 4.3: Figure show numerical result of diffusion coefficient (4.21). This was test for the numerical experiment shown in Fig. 4.2.

We conclude that our equation is more problematic compared to one in [WSS01] due to bad diffusion coefficient which is negative over all interval. We have pure backward nonlinear heat equation, which for sure blows up.

4.2.3 Self-Similarity solutions

In the following subsection we analyse the Eq. (4.11) with the use of self similarity approach.

We suppose that solution of the equation (4.11) has the form

$$u(x,t) = t^{\alpha}\phi(\xi), \quad \text{with} \quad \xi = xt^{\beta}. \tag{4.22}$$

If we plug (4.22) into (4.11) we derive the equation which could be the candidate for the second order ODE under some condition

$$\frac{\alpha}{\lambda}t^{\alpha-1-2\beta}\phi + \frac{\beta}{\lambda}t^{\alpha-1-2\beta}\xi\frac{d\phi}{d\xi} - \left(\frac{\frac{d\phi}{d\xi}}{\phi}\right)^2 + \frac{\frac{d^2\phi}{d\xi^2}}{\phi} = 0.$$

Fixing α and β with relation

$$\alpha = 2\beta + 1,$$

we can reduce (4.11) to the second order ODE

$$\phi\frac{d^2\phi}{d\xi^2} + \left(a_1\xi\phi^2 - \frac{d\phi}{d\xi}\right)\frac{d\phi}{d\xi} + a_2\phi^3 = 0, \tag{4.23}$$

with a_1 and a_2 to be

$$a_1 = \frac{\beta}{\lambda},$$
$$a_2 = \frac{2\beta+1}{\lambda}.$$

Considering the well posed problem of differential equations, one of the criteria is also the boundness (stability) of the solution. If we pretend that the solution (4.22) should be bounded, then the factor α must not be positive

$$\alpha = 2\beta + 1 \leq 0 \quad \rightarrow \quad \beta \leq -\frac{1}{2},$$

and $\phi(\xi)$ must be bounded. As we will show, the PDE (4.11) has a symmetry which fulfils the case of $\beta = -1/2$, but $\phi(\xi)$ is not bounded.

Let us analyse equation (4.23). If we write equation (4.23) as the system of first order ODE's, then we have

$$\begin{aligned} \dot{y_1} &= y_2, \\ \dot{y_2} &= \frac{y_2}{y_1} - a_1 t\, y_1 y_2 - a_2 y_1^2, \end{aligned} \tag{4.24}$$

where we have defined

$$\begin{aligned} t &:= \xi, \\ y_1 &:= \phi, \\ y_2 &:= \frac{d\phi}{d\xi}, \\ \dot{y_2} &:= \frac{d^2\phi}{d\xi^2}. \end{aligned}$$

System (4.24) is non-autonomous and has one fix point $(0, 0)$. If we linearise the system (4.24) around the fix point $(y_1 = 0, y_2 = 0)$ we obtain the system

$$\begin{aligned} \dot{y_1} &= y_2, \\ \lim_{y_1^0 \to 0} \dot{y_2} &= \lim_{y_1^0 \to 0} \frac{y_2}{y_1^0} = \infty, \end{aligned}$$

which shows that the point $(y_1 = 0, y_2 = 0)$ is unstable and leading to singularity in $\phi(\xi)$. Equation (4.11) represents the evolution equation for the shear stress. Shear stress is a nonnegative quantity $u(x, t) \geq 0$, and following the self similarity anzatz (4.22) the quantity y_2 is also a nonnegative $y_2(t) \geq 0$. From numerical solution (Fig. 4.4) we observe that solution explodes for certain initial conditions and values of parameters λ and β. Moreover, model is designed to sustain slow dense granular flow, but the numerical solution predicts quite high shear stress. We conclude, that the model will work only for moderate values of a shear stress. For the case of "big" shear stress, numerical solution will explode.

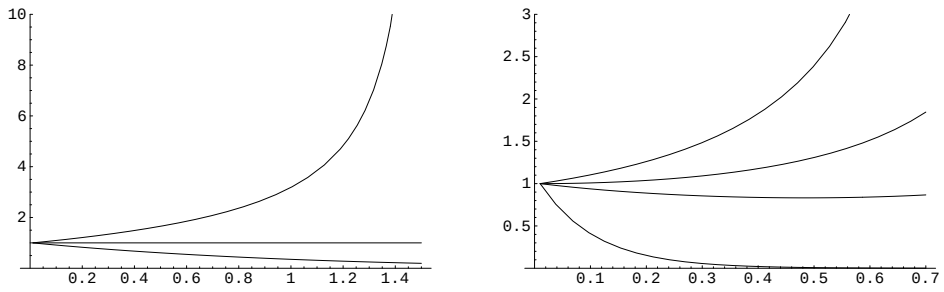

Figure 4.4: Figure shows the numerical solution of (4.23) for $\phi(0) = 1$, $\lambda = 1$ Left: $\beta = -0.5$, $\phi'(0) = 1, 0, -1$, Right: $\beta = -1.5$, $\phi'(0) = 1, 0, -0.7, -1$

As we will see after for the case $\beta = -1/2$ solution always explodes.

The next approach to the solution we used is the method of Lie group of transformations. Nonlinear Parabolic Equation (4.11)

$$\frac{\partial}{\partial t}u = -\lambda\frac{\partial^2}{\partial y^2}(\log u),$$

is a prototype equation for the evolution of a shear stress $u = \frac{\partial v}{\partial y}$. We define domain as an half-plain (see Fig. 4.5).

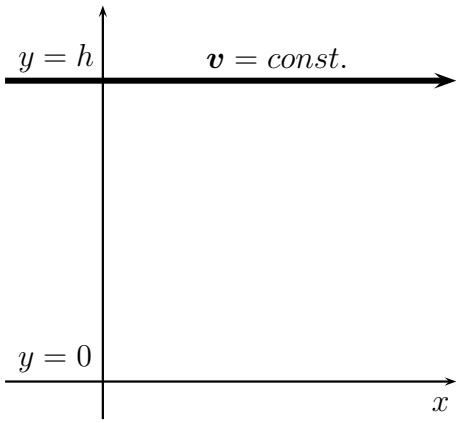

Figure 4.5: Figure shows the domain for the equation (4.11). Boundary at $y = 0$ is fixed - wall, and the boundary at $y = h$, where $h = \infty$ has constant velocity. The x coordinate extends $x \in [-\infty, \infty]$.

Boundary conditions at the wall side ($y = 0$) are:

$$\begin{aligned} u(y = 0, t) &= \tau_0, \quad \text{NO SLIP condition} \\ u(y = 0, t) &= 0, \quad \text{SLIP condition.} \end{aligned} \tag{4.25}$$

By the NO SLIP condition we mean, that the fluid sticks to the wall and SLIP condition means that the fluid has NO friction at the wall [Bat67].

Initial condition must satisfy the condition

$$\int_0^\infty u(y, t = 0)dy < \infty. \tag{4.26}$$

If we analyse Lie groups of transformation of the equation (4.11) we find out that there are 7 infinitesimals

$$
\begin{aligned}
\mathsf{X}_1 &= \frac{\partial}{\partial y}, \quad \text{translation in } y \text{ direction},\\
\mathsf{X}_2 &= \left(y^2 - 2\lambda\frac{t}{u}\right)\frac{\partial}{\partial y} - 4yu\frac{\partial}{\partial u},\\
\mathsf{X}_3 &= \frac{\partial}{\partial t}, \quad \text{translation in } t \text{ direction},\\
\mathsf{X}_4 &= \frac{y}{2}\frac{\partial}{\partial y} + t\frac{\partial}{\partial t}, \quad \text{dilation in } y \text{ and } t,\\
\mathsf{X}_5 &= -\frac{y}{2}\frac{\partial}{\partial y} + u\frac{\partial}{\partial u}, \quad \text{dilation in } y \text{ and } u,\\
\mathsf{X}_6 &= 4\lambda t\frac{\partial}{\partial y},\\
\mathsf{X}_7 &= \left(9\lambda ty - \frac{1}{6}y^3u\right)\frac{\partial}{\partial y} + 8\lambda t^2\frac{\partial}{\partial t} + \left(y^2u^2 - 2\lambda tu\right)\frac{\partial}{\partial u}.
\end{aligned}
\tag{4.27}
$$

There is a 7 parameter Lie group of transformations for the (4.11). In our analysis we will use just the X_4 infinitesimal.

Infinitesimal $\mathsf{X}_4 = \frac{y}{2}\frac{\partial}{\partial y} + t\frac{\partial}{\partial t}$ defines a dilation transformation

$$
\begin{aligned}
\tilde{y} &= e^a y,\\
\tilde{t} &= e^{2a} t,\\
\tilde{u} &= u,
\end{aligned}
\tag{4.28}
$$

and a characteristic system for X_4 is

$$
\frac{dy}{y} = \frac{dt}{2t}. \tag{4.29}
$$

Proposition 4.2.1. *The transformation* (4.28) *leaves the complete problem of equation* (4.11) *invariant.*

Proof: To prove the invariance of the complete problem we have to check the invariance of equation (4.11), domain and boundary conditions. For the shake of simplicity, we will denote the derivatives with the lower indices

$$
\frac{\partial u}{\partial x} = u_x.
$$

(1) equation (4.11):

$$\tilde{u}_{\tilde{t}} = \lambda\left(\frac{\tilde{u}_{\tilde{x}}^2}{\tilde{u}^2} - \frac{\tilde{u}_{\tilde{x}\tilde{x}}}{\tilde{u}}\right)$$
$$e^{-2a}u_t = e^{-2a}\lambda\left(\frac{u_x^2}{u^2} - \frac{u_{xx}}{u}\right)$$
$$u_t = \lambda\left(\frac{u_x^2}{u^2} - \frac{u_{xx}}{u}\right).$$

(2) domain :

$$y = \infty, \quad \tilde{y} = e^a y = e^a \infty = \infty,$$
$$y = 0, \quad \tilde{y} = e^a y = e^a 0 = 0.$$

(3) boundary conditions:

$$u = \tau_0, \quad \tilde{u} = u = \tau_0,$$
$$u = 0, \quad \tilde{u} = u = 0.$$

■

From (4.29) we obtain a new variable by integration

$$\ln y = \ln\sqrt{t} + \ln\xi \quad \rightarrow \quad \xi = \frac{y}{\sqrt{t}}, \tag{4.30}$$

In the new coordinates the solution will have new form $u = \phi(\xi)$ and the (4.11) is reduced to the second order ODE

$$\phi\frac{d^2\phi}{d\xi^2} - \frac{d\phi}{d\xi}^2 - \frac{\xi}{2\lambda}\phi^2\frac{d\phi}{d\xi} = 0. \tag{4.31}$$

If we compare (4.31) and (4.23), we see that (4.31) is a special case of (4.23) for $\beta = -\frac{1}{2}$. Calculating the infinitesimals of (4.31) we get one vector field

$$\mathsf{X} = -\frac{\xi}{2}\frac{\partial}{\partial\xi} + \phi\frac{\partial}{\partial\phi}, \tag{4.32}$$

which generates the next prolongated characteristic system

$$\frac{d\xi}{-\frac{\xi}{2}} = \frac{d\phi}{\phi} = \frac{d\phi_\xi}{\frac{3}{2}\xi\phi}. \tag{4.33}$$

Integrating the system (4.33), we obtain the following coordinate transformations

$$\begin{aligned} x &= \frac{1}{\xi^2\phi}, \\ y &= \frac{\phi^{3/2}}{\phi_\xi}. \end{aligned} \tag{4.34}$$

Inserting the transformations (4.34) in (4.31) we obtain the reduced first order ODE

$$\frac{dy}{dx} = \frac{\frac{1}{\lambda}y^2 - y\sqrt{x}}{4yx^2 + 2x^{3/2}}, \tag{4.35}$$

which has singularity in $x = 0$. For example, if we would replace the transformation (4.30) with

$$\xi = \frac{x}{\sqrt{2\lambda t}}, \tag{4.36}$$

then the second order ODE (4.31) would not have any more the parameter λ, and the first order ODE (4.35) would be

$$\frac{dy}{dx} = \frac{y^2 - y\sqrt{x}}{4yx^2 + 2x^{3/2}}. \tag{4.37}$$

We see that the parameter λ plays a role in the dilation of the coordinate ξ. The phase space of solution would look the same, so from the dynamical system perspective parameter λ doesn't play any crucial role and for the further studies we can write the equation without the parameter λ. But, on a contrary, if λ would be a function of something, it could have influence in the regularisation of Eq. (4.11).

By the author knowledge, ODE (4.35) does not have an analytic solution. As we can see, it has a singularty in the origin $x = 0$. We are again faced with the strong illness of the Eq. (4.11) similar to the one mentioned in [Sch87]

$$\frac{\partial u}{\partial t} = \frac{\partial^2 u}{\partial x^2} - \frac{\partial^2 u}{\partial y^2}.$$

If we linearise Eq. (4.10) around the stationary state solution

$$u(y,t) = ay + w(y,t),$$

we obtain the similar result for the y coordinte

$$\frac{\partial w}{\partial t} = -\alpha \frac{\partial^2 w}{\partial y^2}.$$

We conclude, that dynamic PDE's for slow dense granular flow in dimensions greater than one ($d > 1D$) are very ugly, actually are ill-posed.

Part II – Numerics

Chapter 5

FEM for SDGF 2D Model

Present chapter is devoted to the numerical study of stationary incompressible SDGF. Domain is set in the space between two cylinders.

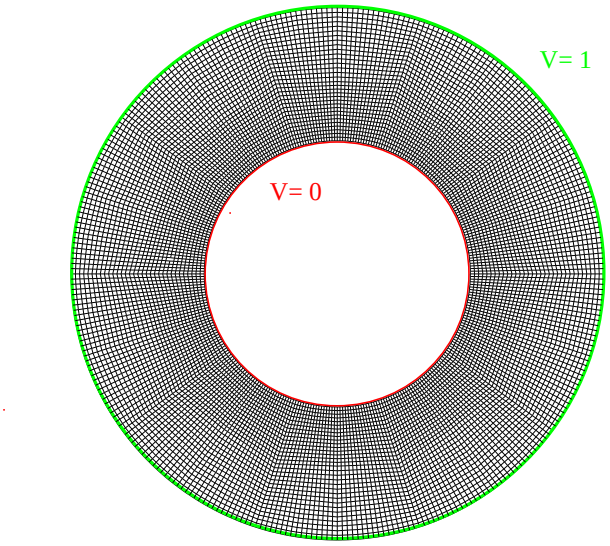

Figure 5.1: Figure show geometry of the computational domain. Inner cylinder has velocity $v = 0$ and outer cylinder has velocity $v = 1$.

We will use standard $Q2/P1$ finite element method. Implementation is done in Deal.II finite element library [BHK]. Code implementation is checked on the stationary incompressible Navier-Stokes system of equations.

The aim of this chapter is to simulate stationary flow, which solution could be compared with the solution of stationary nonlinear parabolic PDE (4.11)

$$\lim_{t\to\infty} u(t, y) = U(y),$$

where $u(t, y)$ is the solution of (4.11). For radially symmetric geometries for small velocities and velocity gradients, we can approximate model equations as to be radially symmetric $u(t, r, \phi) = u(t, r, \phi + \alpha), \forall \alpha$. In this case we can compare numerical solution with the estimates we did in chapter 4.

5.1 Mathematical model

As mentined above, we will simulate Stokes problem

$$\begin{aligned} \nabla \cdot \mathbf{T} &= 0, \\ \nabla \cdot \boldsymbol{v} &= 0, \end{aligned}$$

in a Couette geometry, for two different fluids. First fluid is incompressible Navier-Stokes fluid with constitutive relation

$$\mathbf{T} = -p\mathbf{I} + \frac{1}{Re}\mathbf{D},$$

and the equations of motion are

$$\begin{aligned} \nabla \cdot \left(-p\mathbf{I} + \frac{1}{Re}\mathbf{D} \right) &= 0, \\ \nabla \cdot \boldsymbol{v} &= 0, \end{aligned} \tag{5.1}$$

The second fluid is incompressible SDGF (2.43) with the following constitutive relation

$$\mathbf{T} = p\mathbf{I} + \sqrt{2}\sin\phi \frac{p}{\|\mathbf{D}\| + \epsilon}\mathbf{D},$$

and the equations of motion are

$$\begin{aligned} \nabla \cdot \left(p\mathbf{I} + \sqrt{2}\sin\phi \frac{p}{\|\mathbf{D}\| + \epsilon}\mathbf{D} \right) &= 0, \\ \nabla \cdot \boldsymbol{v} &= 0, \end{aligned} \tag{5.2}$$

where we define $\mathbf{D}$ in (2.29) as strain rate and introduce a regularisation with the parameter ϵ.

We can solve model (5.1) analytically if we introduce cylindrical coordinates. Writing outer radius to be R_1 and inner to be R_2 with boundary conditions $v(R_1) = 1$ and $v(R_2) = 0$ we find the solution to be

$$v(r) = \frac{R_1}{R_2^2 - R_1^2} \frac{R_2^2 - r^2}{r}. \tag{5.3}$$

Fixing $R_1 = 1$ and $R_2 = 0.5$ we have velocity profile

$$v(r) = \frac{4}{3} \frac{1 - r^2}{r}, \quad r \in [\frac{1}{2}, 1]. \tag{5.4}$$

shown on the Fig. 5.2.

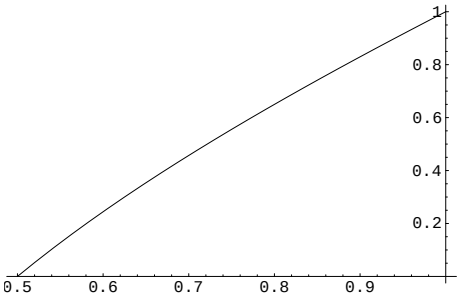

Figure 5.2: Plot of the equation (5.4).

5.2 Numerical method

Numerical method is a standard finite element method for incompressible flows $Q2/P1$, which means that we use Legendre elements of order 2 for velocity and of order 1 for pressure. $Q2/P1$ elements are conforming, meaning that they are globally continuous.

Model (5.1) is linear and can be solved in one step. On a contrary model (5.2) is nonlinear and is linearised using Newton's method.

To formulate a finite element method we need a weak form of the system (5.1) and (5.2). Fortunately this has been already done in [Oua05] and articles mentioned in. Let us state the weak problem:

Weak Problem: *Find* $(\boldsymbol{v}, p) \in X \times M$ *such that*

$$\int_\Omega 2\nu(\|\mathbf{D}(\boldsymbol{v})\|, p)\,\mathbf{D}(\boldsymbol{v}) : \mathbf{D}(\boldsymbol{w})dx + \int_\Omega p\nabla\cdot\boldsymbol{w}dx + \int_\Omega q\nabla\cdot\boldsymbol{v}dx = 0, \quad \forall \boldsymbol{w} \in X = [H_0^1(\Omega)]^2 \quad \forall q \in M = L^2(\Omega), \tag{5.5}$$

where we define

1. *Navier-Stokes fluid:* $\nu(\|\mathbf{D}(\boldsymbol{v})\|, p) = \frac{1}{Re}$
2. *Generalised Navier-Stokes fluid (SDGF):* $\nu(\|\mathbf{D}(\boldsymbol{v})\|, p) = \sqrt{2}\sin\phi\frac{p}{\|\mathbf{D}(\boldsymbol{v})\|+\epsilon}$.

5.2.1 Newton's linearisation

In this approach, the nonlinearity is first handled on the continuous level. Let $\boldsymbol{v}^k, p^k$ be the initial states, then the continuous Newton method consist of finding $\boldsymbol{v}, p$ such that

$$\begin{aligned}\int_\Omega 2\nu(\|\mathbf{D}(\boldsymbol{v}^k)\|, p^k)\mathbf{D}(\boldsymbol{v}) : \mathbf{D}(\boldsymbol{w})dx + \int_\Omega 2\nu(\|\mathbf{D}(\boldsymbol{v}^k)\|, p^k)\mathbf{D}(\boldsymbol{v}^k) : \mathbf{D}(\boldsymbol{w})dx \\ + \int_\Omega 2\partial_1\nu(\|\mathbf{D}(\boldsymbol{v}^k)\|, p^k)\left[\mathbf{D}(\boldsymbol{v}^k) : \mathbf{D}(\boldsymbol{v})\right]\left[\mathbf{D}(\boldsymbol{v}^k) : \mathbf{D}(\boldsymbol{w})\right]dx \\ + \int_\Omega 2\,p\,\partial_2\nu(\|\mathbf{D}(\boldsymbol{v}^k)\|, p^k)\left[\mathbf{D}(\boldsymbol{v}^k) : \mathbf{D}(\boldsymbol{w})\right]\,dx = 0, \quad \forall \boldsymbol{w} \in W, \\ \int_\Omega q\nabla\cdot\boldsymbol{v}\,dx = 0, \quad \forall q \in P,\end{aligned} \tag{5.6}$$

where $\partial_i\nu,\ i = 1, 2$, is the partial derivative of ν related to the first and second variable. The resulting auxiliary subproblem in each Newton step consist of finding $\boldsymbol{v}, p \in X \times M$ as solution of linear (discretised) system

$$\begin{cases} A(\boldsymbol{v}^k, p^k)\boldsymbol{v} + \delta_a A^*(\boldsymbol{v}^k, p^k)\boldsymbol{v} + Bp + \delta_b B^*(\boldsymbol{v}^k, p^k)p = R_{\boldsymbol{v}}(\boldsymbol{v}^k, p^k), \\ B^\mathsf{T}p = R_p(\boldsymbol{v}^k, p^k), \end{cases} \tag{5.7}$$

where $R_{\boldsymbol{v}}(\cdot,\cdot)$ and $R_p(\cdot,\cdot)$ denote the corresponding nonlinear residual terms for the momentum and continuity equation and the operators $A(\boldsymbol{v}^k, p^k)$, B, $A^*(\boldsymbol{v}^k, p^k)$ and $B^*(\boldsymbol{v}^k, p^k)$ are defined as follows:

$$\begin{aligned}
\langle A(\boldsymbol{v}^k, p^k)\boldsymbol{v}, \boldsymbol{w}\rangle &= \int_\Omega 2\nu(\|\mathbf{D}(\boldsymbol{v}^k)\|, p^k)\mathbf{D}(\boldsymbol{v}) : \mathbf{D}(\boldsymbol{w})dx,\\
\langle Bp, \boldsymbol{w}\rangle &= \int_\Omega p\nabla\cdot\boldsymbol{w}\, dx,\\
\langle A^*(\boldsymbol{v}^k, p^k)\boldsymbol{v}, \boldsymbol{w}\rangle &= \int_\Omega 2\partial_1\nu(\|\mathbf{D}(\boldsymbol{v}^k)\|, p^k)\left[\mathbf{D}(\boldsymbol{v}^k) : \mathbf{D}(\boldsymbol{v})\right]\left[\mathbf{D}(\boldsymbol{v}^k) : \mathbf{D}(\boldsymbol{w})\right] dx,\\
\langle B^*(\boldsymbol{v}^k, p^k)\boldsymbol{w}, p\rangle &= \int_\Omega 2\, p\, \partial_2\nu(\|\mathbf{D}(\boldsymbol{v}^k)\|, p^k)\left[\mathbf{D}(\boldsymbol{v}^k) : \mathbf{D}(\boldsymbol{w})\right]\, dx\\
\langle Bq, \boldsymbol{v}\rangle &= \int_\Omega q\nabla\cdot\boldsymbol{v}\, dx.
\end{aligned} \tag{5.8}$$

For the case of $\delta_a = \delta_b = 0$ we have ***fixpoint method*** and for the case $\delta_a = \delta_b = 1$ we have ***full Newton's method***. We obtain the solution in the iteration procedure as

$$(\boldsymbol{v}^{l+1}, p^{l+1}) = (\boldsymbol{v}^l, p^l) + \omega^l(\boldsymbol{v} - \boldsymbol{v}^l, p - p^l),$$

where $\omega^l \in [-1, 0)$ and $(\boldsymbol{v}, p)$ is the solution vector of the linear system (5.7). The end of iteration is defined with the prescribed error in L^2 norm as

$$\mathrm{Err}_{L^2} = \|(\boldsymbol{v}^{l+1}, p^{l+1}) - (\boldsymbol{v}^l, p^l)\|_{L^2}.$$

We would usually prescribe the error value as $\mathrm{Err}_{L^2} \approx 10^{-8}$.

Remark. In the upper iteration procedure we have defined the correction vector as a difference in the computed solution and the solution in the previous time step

$$(\boldsymbol{v} - \boldsymbol{v}^l, p - p^l).$$

We used this definition to preserve the boundary conditions, because then the correction vector has values 0 on the boundary.

5.3 Results

In this section we will show numerical results for both models, Newtonian fluid and SDGF. Solution of the nonlinear problem is obtained by two iteration procedures. The first one is fixedpoint method, and the second one is full Newton's method.

5.3.1 Newtonian fluid

Code implementation is tested with the Newtonian fluid model (5.1), for which we already know the analytical solution. For the solution of linear system we used BicgStab method with the convergence error criteria to be $eps = 10^{-8}$. Domain was parcelled on 7424 cells with 69136 degrees of freedom. BicgStab iteration needed 206 steps to reach desiderate error. Fig. 5.3 show numerical results. If we compare analytical solution (5.4) and the radial cutline of numerical solution in Fig. 5.4 we see that results are identical. This confirms that the implementation is correct.

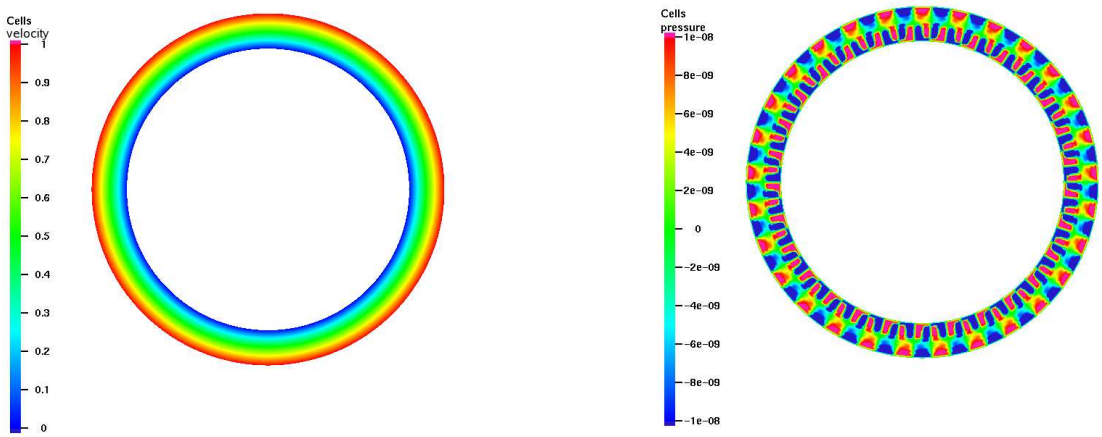

Figure 5.3: Solution of Newtonian fluid for $Re = 10$.

5.3.2 SDGF fluid

Now we show results for the SDGF (5.2). We used a regularisation parameter ε to avoid singularities in the places of the zero velocity gradients. Value of ε is always fixed at the value 10^{-8}. We observe, that small changes in ε do not contribute to the change in solutions.

We used two linearisation procedures to solve the problem. Fixpoint and full Newton's method. In fixpoint method we do not take into account the derivatives but the full Newton's method does. More complicated bilinear forms made linear system more complicated and harder to solve.

5.3.2.1 Fixpoint method

In the Figs. 5.5, 5.6, 5.7 and tables 5.1, 5.2 and 5.3 are results of the numerical solution obtained with fixpoint method. For the boundary layer solutions we had problems with the convergency in BicgStab method. Linear system must have very bad properties. In the Fig. 5.4 we have the radial cutline velocity profile for all four solutions.

We see that the analytical prediction (5.4) and numerical result fits completely for the newtonian fluid and confirms the correct implementation. Moreover, there are three solutions for which the error in L^2 norm decreases and in some sense gives us the convergency test. This confirms the numerical existence of three possible solutions for the steady state SDGF equation in a Couette flow regime. In the tables 5.1, 5.2 and 5.3 we show the iteration data for all three solutions.

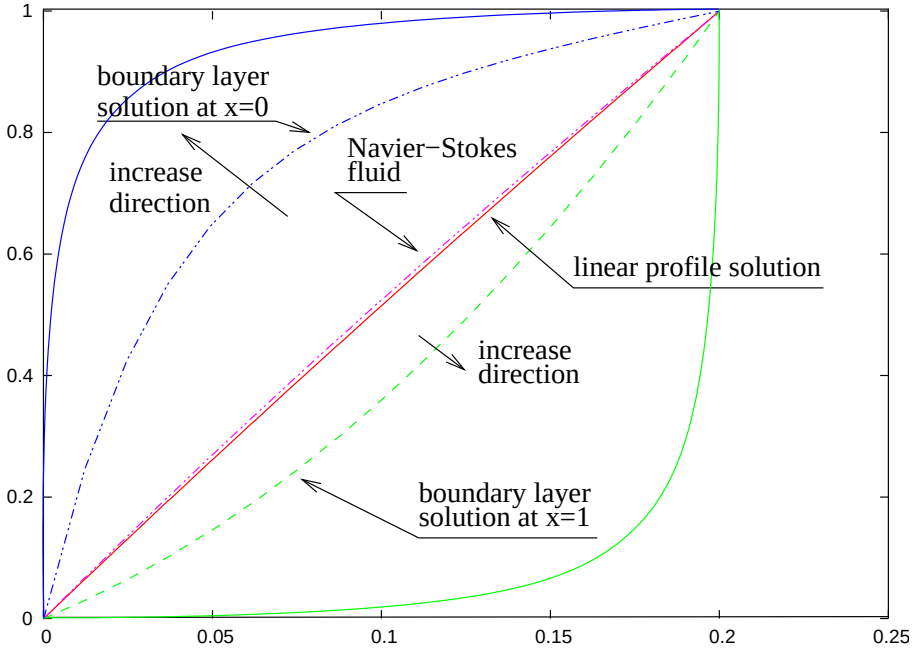

Figure 5.4: Radial cutline velocity profiles of figures 5.5, 5.6, 5.7. On x axis we plot radial distance from inner cylinder to outer cylinder and on the y axis we plot the velocity amplitude $v = \sqrt{v_x^2 + v_y^2}$. The solid blue and green lines shows how solution should increase if the convergence of a BicgStab method would not fail. Solution of Newtonian fluid was taken for the initial iterative value $(\boldsymbol{v}^0, p^0)$.

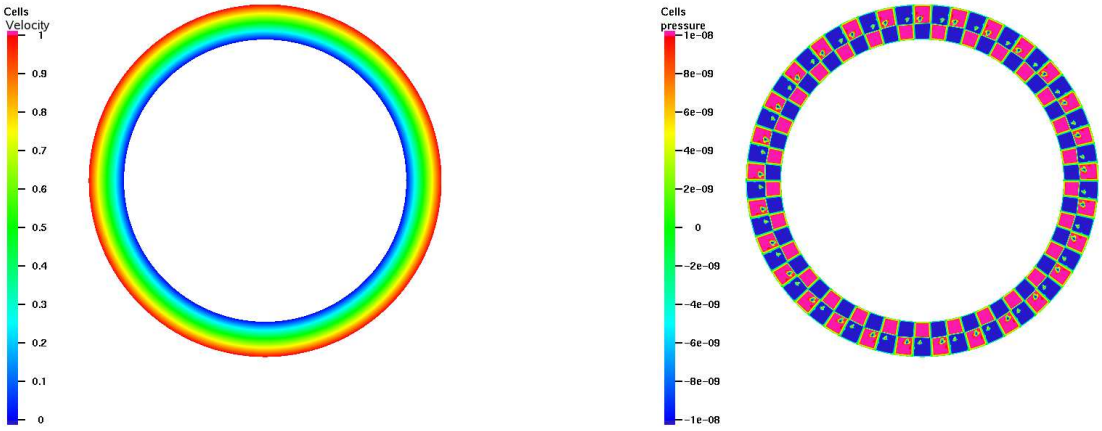

Figure 5.5: Figure show velocity and pressure for linear solution in 27th iteration step with $\mathrm{Err}_{L^2} = 9.15\,10^{-9}$.

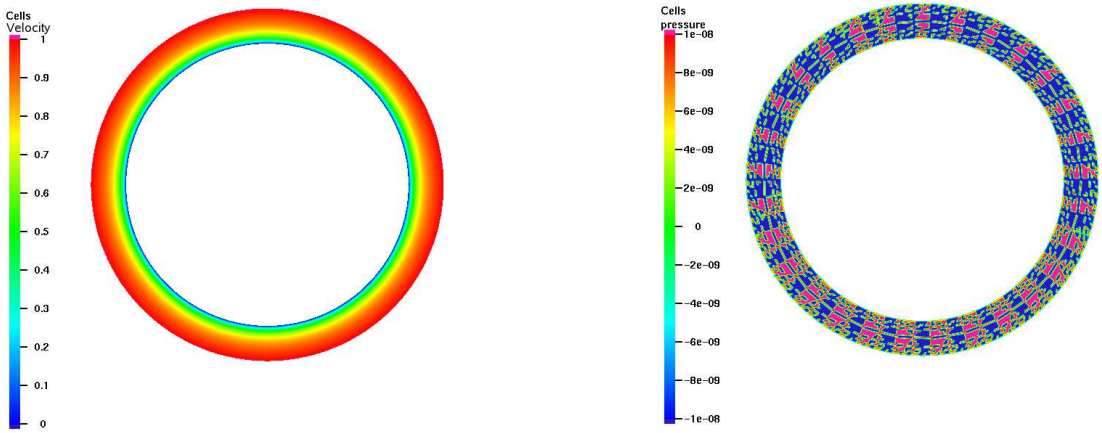

Figure 5.6: Figure show velocity and pressure for boundary layer solution at $x = 0$ in 11th iteration step with $\mathrm{Err}_{L^2} = 2.34$.

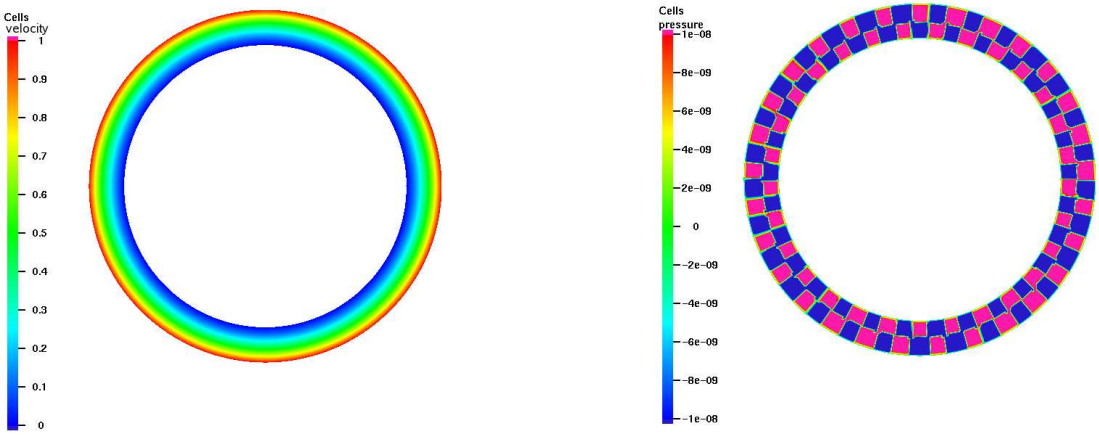

Figure 5.7: Figure show velocity and pressure for boundary layer solution at $x = 1$ in 10th iteration step with $\mathrm{Err}_{L^2} = 1.34$.

Table 5.1: Data of convergency for fixpoint method – boundary layer at $x = 0$. Method did not converged, BicgStab steps passed the limit of 5000 iterations.

Iter. step l	BicgStab steps	BicgStab err	damping ω^l	Err_{L^2}
0	197	1e-08	0.900000	5.499900e+00
1	667	1e-08	0.900000	5.307006e+00
2	559	1e-08	0.900000	5.054617e+00
3	605	1e-08	0.900000	4.758089e+00
4	550	1e-08	0.900000	4.433567e+00
5	601	1e-08	0.900000	4.096267e+00
6	832	1e-08	0.900000	3.759242e+00
7	1422	1e-08	0.900000	3.432737e+00
8	1561	1e-08	0.900000	3.124043e+00
9	1579	1e-08	0.900000	2.837733e+00
10	2065	1e-08	0.900000	2.576109e+00
11	3236	1e-08	0.900000	2.339728e+00

Table 5.2: Data of convergency for fixpoint method – boundary layer at $x = 1$. Method did not converged, BicgStab steps passed the limit of 5000 iterations.

Iter. step l	BicgStab steps	BicgStab err	damping ω^l	Err_{L^2}
0	197	1e-08	0.900000	5.499900e+00
1	207	1e-08	0.450000	2.783601e+00
2	221	1e-08	0.225000	1.394552e+00
3	318	1e-08	0.225000	1.394479e+00
4	453	1e-08	0.225000	1.393157e+00
5	535	1e-08	0.225000	1.390588e+00
6	426	1e-08	0.225000	1.386782e+00
7	869	1e-08	0.225000	1.381753e+00
8	908	1e-08	0.225000	1.375522e+00
9	1152	1e-08	0.225000	1.368116e+00
10	1882	1e-08	0.225000	1.359565e+00

5.3.2.2 Full Newton's method

Full Newton's method includes two extra bilinear forms from nonlinear operators A^* and B^* from the system (5.8).

In fixpoint method we were able to obtain desirous convergence just for the linear velocity profile, but for the boundary layer solutions BiCGStab method failed to solve linear system. Matrix is to stiff to be solved by the ordinary solvers and needs advanced approach.

In full Newton's method system matrix of linear system is even more stiff and BiCGStab mathod fails in the second iteration step.

We conclude, that SDGF model, which is nonlinear, produce very stiff matrices. Standard methods like GMRES, BiCGStab do not converge to small errors. It is a high need to introduce advanced linear iterative solvers to solve SDG flow.

Table 5.3: Data of convergency for fixpoint method – linear profile. Method ended with desiderate precision of err_{L^2}.

Iter. step l	BicgStab steps	BicgStab err	damping ω^l	Err_{L^2}
0	197	1e-08	0.100000	6.111000e-01
1	221	1e-08	0.050000	3.063159e-01
2	230	1e-08	0.025000	1.533423e-01
3	187	1e-08	0.012500	7.671634e-02
4	184	1e-08	0.006250	3.836935e-02
5	240	1e-08	0.003125	1.918746e-02
6	221	1e-08	0.001563	9.594423e-03
7	230	1e-08	0.000781	4.797385e-03
8	235	1e-08	0.000391	2.398736e-03
9	193	1e-08	0.000195	1.199379e-03
10	229	1e-08	0.000098	5.996920e-04
11	220	1e-08	0.000049	2.998467e-04
12	218	1e-08	0.000024	1.499235e-04
13	237	1e-08	0.000012	7.496180e-05
14	171	1e-08	0.000006	3.748091e-05
15	176	1e-08	0.000003	9.370229e-06
17	176	1e-08	0.000001	4.685115e-06
18	270	1e-08	0.000000	2.342557e-06
19	223	1e-08	0.000000	1.171279e-06
20	186	1e-08	0.000000	5.856394e-07
21	174	1e-08	0.000000	2.928197e-07
22	228	1e-08	0.000000	1.464098e-07
23	175	1e-08	0.000000	7.320492e-08
24	223	1e-08	0.000000	7.320492e-08
25	227	1e-08	0.000000	3.660246e-08
26	245	1e-08	0.000000	9.150615e-09

Chapter 6

RKDG FEM for Antiplane Shear Model

In this chapter, we will introduce the elasto-plastic model derived by D. G. Schaeffer [Sch92]. It will be shown that the system of PDE's is hyperbolic under some conditions. We will use Runge Kutta Discontinuous Galerkin Finite Element Method to solve the model.

6.1 Mathematical model

Physically the model may be visualised as antiplane shearing with a somewhat artificial constitutive law. The flow of granular material is discussed in terms of a continuum model. Model restricts its attention in two space variables x_1, x_2 and time t. The unknown functions consist of the scalar density ρ, the velocity vector $\boldsymbol{v}$ and the Cauchy stress tensor $\mathbf{T}$. These quantities are subject to conservation of mass as momentum

$$\begin{aligned} \frac{\mathrm{D}\rho}{\mathrm{D}t} + \rho\frac{\partial v_i}{\partial x_i} &= 0, \\ \rho\frac{\mathrm{D}v_i}{\mathrm{D}t} + \frac{\partial \mathsf{T}_{ij}}{\partial x_j} &= 0, \end{aligned} \tag{6.1}$$

where summation convention is assumed. We use phenomenological constitutive relations of the elastoplastic type with response function determined from experiments. In this kind of constitutive relation, one distinguishes between elastic (reversible) and plastic (irreversible) deformation. Following the usual terminology, we shall say the material is ***loading*** if the deformation includes plastic

strains, otherwise is ***unloading***. Since the response of the material in loading or unloading is quite different, we have a constitutive law with two cases

$$\frac{d\mathsf{T}_{ij}}{dt} = \begin{cases} L_{ijkl}(\mathbf{T})\frac{\partial v_l}{\partial x_k}, & \text{if loading,} \\ M_{ijkl}(\mathbf{T})\frac{\partial v_l}{\partial x_k}, & \text{if unloading.} \end{cases} \tag{6.2}$$

The model we consider has three unknowns. Altough the model is formulated in purely two-dimensional terms, it may be losely interpreted in three dimensions as ***antiplane shearing***. The three unknowns consist of a scalar velocity v, which corresponds to the x_3-component of the full velocity vector $\boldsymbol{v}$, and a stress vector $\boldsymbol{\tau} = (\tau_1, \tau_2)$, which coresponds to the T_{31}, T_{32} components of the full stress tensor. Density and other components of the stress are constant, and the other components of velocity vanish; the three unknown functions depend on x_1, x_2, t but not on x_3.

Remark. The equations of antiplane shearing are simpler because the Eulerian and Lagrangian representation conicides.

We give the equations of the model in non-dimensional form

$$c_e^{-2}\frac{\partial v}{\partial t} = \nabla \cdot \boldsymbol{\tau}, \tag{6.3a}$$

$$\left(\mathbf{I} + \frac{1}{h(\|\boldsymbol{\tau}\|)}(\mathbf{R}\boldsymbol{\tau})\boldsymbol{\tau}^{\mathsf{T}}\right)\frac{\partial \boldsymbol{\tau}}{\partial t} = \nabla v, \quad \text{if loading.} \tag{6.3b}$$

$$\frac{\partial \boldsymbol{\tau}}{\partial t} = \nabla v, \quad \text{if unloading.} \tag{6.3c}$$

Here c_e is a constant, the speed of elastic waves

$$c_e = \sqrt{\frac{G}{\rho}}\frac{L}{T};$$

$\mathbf{I}$ is the 2×2 identity matrix; $\mathbf{R}$ is the rotation matrix

$$\mathbf{R} = \begin{pmatrix} \cos\alpha & \sin\alpha \\ -\sin\alpha & \cos\alpha \end{pmatrix},$$

where $\alpha \in (0, \frac{1}{2}\pi)$ is a parameter characterising the degree of non-associativity; and $h(\|\boldsymbol{\tau}\|)$ is the hardening modulus, a positive monotone decreasing function on the interval $\|\boldsymbol{\tau}\| \in [0, 1]$ which vanishes at $\|\boldsymbol{\tau}\| = 1$. Typical dimensions in the experiment of Vardulakis & Graf [VG85] were

$L = 10\text{cm}$, $U = 2\text{mm/h}$, $\tau_{\max} = 10^5\text{Pa}$, $G = 5\,10^6\text{Pa}$, $\rho = 1\text{g/cm}^3$,

and the speed of elastic waves has value $c_e^2 = 6.5\,10^{12}$.

The condition which distinguish the states of loading and unloading is expressed in terms of yield surface. Relative to a given solution $v(x,t)$, $\boldsymbol{\tau}(x,t)$ the yield surface at x,t is the circle

$$\{\boldsymbol{\tau} \in \mathbb{R}^2 : \|\boldsymbol{\tau}\| = \max_{0\le s\le t} \|\boldsymbol{\tau}(x,s)\|\}. \tag{6.4}$$

Note that as time evolves, (6.4) may expand but never contract.

the following lemma precisely defines the state of loading and unloading

Lemma 6.1.1. *Material is loading at x,t if*

$$\|\boldsymbol{\tau}\| = \max_{0\le s\le t} \|\boldsymbol{\tau}(x,s)\|, \quad \textit{and} \tag{6.5a}$$

$$\langle \boldsymbol{\tau}(x,t), \nabla v(x,t)\rangle > 0, \tag{6.5b}$$

otherwise is unloading.

We can rewrite the system (6.3) in quasi linear form. Doing so we obtain

$$\frac{\partial \boldsymbol{u}}{\partial t} + \mathbf{B}_1 \frac{\partial \boldsymbol{u}}{\partial x_1} + \mathbf{B}_2 \frac{\partial \boldsymbol{u}}{\partial x_2} = 0, \tag{6.6}$$

where

$$\boldsymbol{u} = \begin{pmatrix} v \\ \tau_1 \\ \tau_2 \end{pmatrix}, \quad \mathbf{B}_1 = \begin{pmatrix} 0 & c_e^2 & 0 \\ b_{11} & 0 & 0 \\ b_{21} & 0 & 0 \end{pmatrix}, \quad \mathbf{B}_2 = \begin{pmatrix} 0 & 0 & c_e^2 \\ b_{12} & 0 & 0 \\ b_{22} & 0 & 0 \end{pmatrix}$$

with

$$b_{ij} = \delta_{ij} - \frac{(\mathbf{R}\boldsymbol{\tau})_i \tau_j}{h(\|\boldsymbol{\tau}\|) + \|\boldsymbol{\tau}\|^2 \cos\alpha}.$$

Calculating the eigenvalues we find

$$\lambda(\mathbf{B}_1) = \{0, -c_e\sqrt{b_{11}}, c_e\sqrt{b_{11}}\}, \quad \lambda(\mathbf{B}_2) = \{0, -c_e\sqrt{b_{22}}, c_e\sqrt{b_{22}}\}.$$

When the $b_{ii} > 0$ system is hyperbolic. In [Sch92] it is shown, when the system (6.6) loses hyperbolicity, the initial value problem becomes linearly ill-posed (in

the sense of Hadamard). On a contrary the model is nonlinear and the full nonlinear analysis would clarify the question of ill-posed situation. The inclusion of higher-order effects, as for example rate-dependant model, Cosserat structure, cancels out the ill-posed behaviour. If we speculate, the zero-order model is not good after the ignition of the formation of a shear band and can not predict its evolution.

6.2 Numerical method

A conservation law is an equation in divergence form

$$\frac{\partial}{\partial t}\boldsymbol{u} + \nabla \cdot \mathbf{F}(\boldsymbol{u}) + \boldsymbol{f}(\boldsymbol{u}) = 0, \tag{6.7}$$

where

$\boldsymbol{x} \in \mathbb{R}^n$ denotes the independent variables, $\boldsymbol{u} \in \mathbb{R}^m$ denote the dependant variables, $\mathbf{F} : \mathbb{R}^m \to \mathbb{R}^n$ is a flux mapping, $\boldsymbol{f} \in \mathbb{R}^m$ are sources. When the differentiation is carried out, a quasi linear system of first order result in

$$\frac{\partial}{\partial t}\boldsymbol{u}(t,\boldsymbol{x}) + \sum_{i=1}^{n} \mathbf{A}_i \frac{\partial \boldsymbol{u}(t,\boldsymbol{x})}{\partial x_i} + \boldsymbol{f}(\boldsymbol{u}(t,\boldsymbol{x})) = 0. \tag{6.8}$$

Then the system of conservation law is called hyperbolic, if the matrices $\mathbf{A}_i(\boldsymbol{u})$ have real and distinct eigenvalues for all values of argument $\boldsymbol{u}$. By this definition we see that system (6.6) is hyperbolic *iff* $b_{ii} > 0$.

The majority of numerical methods for hyperbolic laws have been developed with equation (6.7) in mind, but the system (6.6) is not in conservative form. The standard numerical methods can not be applied directly to our problem. Therefore we need an extension of standard method to the non-conservative form. We will use ***Runge Kutta Discontinuous Galerkin Finite Element Method (RKDG FEM)*** developed by Cockburn & Shu [CS89a, CS89b, CS90] and extended to the non-conservative form by Hulsen [Hul91]. We choose this particular method, because of its high order and the ability of mesh adaption. As we know, granular flow in its evolution can develop discontinuity named shear bands, and this cause to concentrate the number of discretisation cells near the line (or surface in 3D) of formed shear band. If we would choose very fine grid on a whole domain it would take us enormous computational power to solve the problem. Therefore, with the use of mesh addaption we can avoid such problems and concentrate the computational power merely in the region of fast solution changes (domain where shear band will form).

6.2.1 The DGRK FEM for conservation law in conservative form

We will discretise (6.8) with DG method in space and with explicite RK in time. In the following we divide domain Ω into finite elements $\Omega = \cup_{e=1}^{n}\Omega_e$. On each element Ω_e we approximate solution $\boldsymbol{u}$ with $\boldsymbol{u}_h$, which consist of polynomials of the order l. The approximation is allowed to be discontinuous across the element boundaries $\partial\Omega_e$. We will denote the living space for the approximate solutions by $V_h^{(e)}$.

Let us multiply (6.7) by a test function $\boldsymbol{w}$ and integrating over the domain Ω gives

$$\int_\Omega \boldsymbol{w}(\boldsymbol{x})\left(\frac{\partial}{\partial t}\boldsymbol{u}(t,\boldsymbol{x}) + \nabla\cdot\mathbf{F}(\boldsymbol{u}(t,\boldsymbol{x})) + \boldsymbol{f}(\boldsymbol{u}(t,\boldsymbol{x}))\right)dx = 0, \quad \forall \boldsymbol{w}\in V, \tag{6.9}$$

where V is a suitable function space for both $\boldsymbol{u}$ and $\boldsymbol{w}$, for example $V \subset H^1(\Omega)$. We approximate the space V by $V_h^{(e)}$. Note that $V_h^{(e)}$ is only an approximation of the space V on element level. For the later use we will denote cell Ω_e as K and $V_h^{(e)}$ as $V_h(K)$. Substituting the approximation into (6.9) requires the integral to be splitted into a sum over element integrals and a sum over element boundary integrals. Partial integration of the flux term gives

$$\begin{aligned}\int_K \boldsymbol{w}_h(\boldsymbol{x})\frac{\partial \boldsymbol{u}_h(t,\boldsymbol{x})}{\partial t}dx - \int_K \nabla\boldsymbol{w}_h(\boldsymbol{x}) : \mathbf{F}(\boldsymbol{u}_h)dx + \\ \int_{\partial K}\boldsymbol{w}_h(\boldsymbol{x})\boldsymbol{F}_n(\boldsymbol{u}_h)dl = \int_K \boldsymbol{w}_h(\boldsymbol{x})\boldsymbol{f}(t,\boldsymbol{x})dx, \\ \forall \boldsymbol{w}_h \in V_h(K),\end{aligned} \tag{6.10}$$

where we define the normal flux vector by

$$\boldsymbol{F}_n(\boldsymbol{u}_h) := \mathbf{F}(\boldsymbol{u}_h)\boldsymbol{n},$$

with $\boldsymbol{n}$ being the boundary normal vector pointing outward on ∂K. The coupling beetwen the elements consists of a weak form of boundary conditions for the normal fluxes, which may also be interpreted as specifying a flux expression of the following form

$$\boldsymbol{F}_n(\boldsymbol{u}_h) = \boldsymbol{h}(\boldsymbol{u}_h^-, \boldsymbol{u}_h^+),$$

where we have used the convention that the indices $-$ and $+$ denote the 'backside' and 'frontside' of the normal vector $\boldsymbol{n}$. This convention will be used always.

The function $\boldsymbol{u}_h$ and $\boldsymbol{w}_h$ may be written as follows on an element K

$$\boldsymbol{u}_h(t,\boldsymbol{x}) := \sum_{i=1}^{N} u_i(t)\boldsymbol{\phi}_i(\boldsymbol{x}), \quad \boldsymbol{w}_h(\boldsymbol{x}) := \sum_{i=1}^{N} w_i\boldsymbol{\phi}_i(\boldsymbol{x}),$$

where $\boldsymbol{\phi}_i(\boldsymbol{x})$ are the basis functions and $u_i(t)$ are arbitrary coefficient, which need to be determined. Inserting the upper relations in the (6.10) we get DGFEM for conservation law in conservative form

$$\frac{\partial u_i(t)}{\partial t}\int_K \boldsymbol{\phi}_i\boldsymbol{\phi}_j dx - \int_K \nabla\boldsymbol{\phi}_i : \mathbf{F}(u_j(t)\boldsymbol{\phi}_j)dx + \int_{\partial K} \boldsymbol{\phi}_i\boldsymbol{F}_n(u_j(t)\boldsymbol{\phi}_j)dl = \int_K \boldsymbol{\phi}_i\boldsymbol{f}(t,\boldsymbol{x})dx, \qquad \forall\boldsymbol{\phi}_i \in P_N(K).$$

Writing vector of unknown coefficients as $\boldsymbol{U} = \{u_1(t),\dots,u_N(t)\}$ we can rewrite the upper equation in the matrix form

$$\mathbf{M}\frac{\partial \boldsymbol{U}}{\partial t} - \mathbf{K}(\boldsymbol{U})\boldsymbol{U} + \mathbf{F}(\boldsymbol{U})\boldsymbol{U} = \boldsymbol{g},$$

where $\mathbf{K}(\boldsymbol{U})$ and $\mathbf{F}(\boldsymbol{U})$ are nonlinear operators. Collecting all cells contribution, the upper equation forms the global system of equations for the solution vector $\boldsymbol{U}$. Rewriting the upper system we obtain nonlinear system of ODE's for the coefficients $u_i(t)$

$$\frac{\partial \boldsymbol{U}}{\partial t} = \mathbf{M}^{-1}\left[\mathbf{K}(\boldsymbol{U})\boldsymbol{U} - \mathbf{F}(\boldsymbol{U})\boldsymbol{U} + \boldsymbol{g}\right]. \tag{6.11}$$

If are the basis function $\boldsymbol{\phi}_i$ orthogonal, then the mass matrix $\mathbf{M}$ is diagonal and the inverse is computationally cheap. The equation (6.11) can be solved in a few ways:

(1) ***explicit scheme - linear case***:

$$\frac{\partial \boldsymbol{U}}{\partial t}(\boldsymbol{U}^{k+1},\boldsymbol{U}^k) = \mathbf{M}^{-1}\left[\mathbf{K}(\boldsymbol{U}^k)\boldsymbol{U}^k - \mathbf{F}(\boldsymbol{U}^k)\boldsymbol{U}^k + \boldsymbol{g}\right]$$

(2) ***implicit scheme - linear case***:

$$\frac{\partial \boldsymbol{U}}{\partial t}(\boldsymbol{U}^{k+1}, \boldsymbol{U}^k) = \mathbf{M}^{-1}\left[\mathbf{K}(\boldsymbol{U}^k)\boldsymbol{U}^{k+1} - \mathbf{F}(\boldsymbol{U}^k)\boldsymbol{U}^{k+1} + \boldsymbol{g}\right]$$

(3) ***implicit scheme - nonlinear case***:

$$\frac{\partial \boldsymbol{U}}{\partial t}(\boldsymbol{U}^{k+1}, \boldsymbol{U}^k) = \mathbf{M}^{-1}\left[\mathbf{K}(\boldsymbol{U}^{k+1})\boldsymbol{U}^{k+1} - \mathbf{F}(\boldsymbol{U}^{k+1})\boldsymbol{U}^{k+1} + \boldsymbol{g}\right]$$

We approximate time derivative

$$\frac{\partial \boldsymbol{U}}{\partial t}(\boldsymbol{U}^{k+1}, \boldsymbol{U}^k)$$

with high order Runge-Kutta using Generalised Slope Limiter method.

6.2.2 The DGRK FEM for conservation law in non-conservative form

For the system (6.8) we cannot perform a partial integration to weakly imposed boundary conditions. Multiplying (6.8) by a test function $\boldsymbol{w}$ and integrating over the domain Ω gives

$$\int_K \boldsymbol{w}_h(\boldsymbol{x})\left[\frac{\partial \boldsymbol{u}_h(t,\boldsymbol{x})}{\partial t} + \sum_{i=1}^{d} \mathbf{A}_i(\boldsymbol{u}_h(t,\boldsymbol{x}))\frac{\partial \boldsymbol{u}_h(t,\boldsymbol{x})}{\partial x_i} - \boldsymbol{f}(t,\boldsymbol{x})\right] dx + \int_{\partial K} \boldsymbol{w}_h(\boldsymbol{x})\Delta_n(\boldsymbol{u}_h^+(t,\boldsymbol{x}), \boldsymbol{u}_h^-(t,\boldsymbol{x}), \boldsymbol{n}(\boldsymbol{x}))dl = 0 \tag{6.12}$$

Integration over the boundary of element gives us an extra term due to the jump in the derivative of $\boldsymbol{u}_h$ in the normal direction (component of $\frac{\partial \boldsymbol{u}_h}{\partial x_i}$ in the normal direction is infinite). The extra term is

$$\Delta_n(\boldsymbol{u}_h^+(t,\boldsymbol{x}), \boldsymbol{u}_h^-(t,\boldsymbol{x}), \boldsymbol{n}(\boldsymbol{x})) = \int_{\boldsymbol{u}_h^+}^{\boldsymbol{u}_h^-} \sum_{i=1}^{d} n_i \mathbf{A}_i(\boldsymbol{u}_h)d\boldsymbol{u} = \int_{\boldsymbol{u}_h^+}^{\boldsymbol{u}_h^-} \mathbf{K}_n(\boldsymbol{u}_h)d\boldsymbol{u},$$

where we have

- $\boldsymbol{n}$ is the normal vector on the boundary ∂K,
- $\boldsymbol{u}_h^+$ is a value of $\boldsymbol{u}_h$ on the neighbour element boundary, pointed by $\boldsymbol{n}$,
- $\boldsymbol{u}_h^-$ is a value of $\boldsymbol{u}_h$ on the element boundary.

We can make the jump

$$[\boldsymbol{u}] := \boldsymbol{u}^+ - \boldsymbol{u}^-$$

as small as we wish by the use of mesh adaptivity, then the integral can be approximated by the midpoint rule

$$\Delta_n \approx \mathbf{K}_n(\frac{\boldsymbol{u}^+ + \boldsymbol{u}^-}{2})[\boldsymbol{u}] + \mathcal{O}([\boldsymbol{u}]^2).$$

Summarasing all we derived the method for conservation law in nonconservative form.

$$\begin{aligned}\int_K \boldsymbol{w}_h(\boldsymbol{x}) \left[\frac{\partial \boldsymbol{u}_h(t,\boldsymbol{x})}{\partial t} + \sum_{i=1}^{d} \mathbf{A}_i(\boldsymbol{u}_h(t,\boldsymbol{x}))\frac{\partial \boldsymbol{u}_h(t,\boldsymbol{x})}{\partial x_i} - \boldsymbol{f}(t,\boldsymbol{x})\right] dx \quad + \\ \int_{\partial K} \boldsymbol{w}_h(\boldsymbol{x})\mathbf{K}_n(\frac{\boldsymbol{u}_h^+(t,\boldsymbol{x}) + \boldsymbol{u}_h^-(t,\boldsymbol{x})}{2})[\boldsymbol{u}_h(t,\boldsymbol{x})]dl \quad = \quad 0.\end{aligned}$$

In the same way as for the conservative form, we derive the system of nonlinear ODE's, which we solve with the same approach as for system (6.11).

6.3 Results

The method was implemented in the finite element package DEAL.II [BHK]. In computations we used Discontinuous Legendre Elements of 0^{th} and 1^{st} order with Kelly and Gradient error estimators for the mesh adaptivity. Explicit scheme

$$\frac{\partial \boldsymbol{U}}{\partial t}(\boldsymbol{U}^{k+1}, \boldsymbol{U}^k) = \mathbf{M}^{-1}\left[\mathbf{K}(\boldsymbol{U}^k)\boldsymbol{U}^k - \mathbf{F}(\boldsymbol{U}^k)\boldsymbol{U}^k + \boldsymbol{g}\right]$$

was used for time integration.

6.3.1 Test cases

We have checked the implementation of the method on the linear case

$$\frac{\partial u}{\partial t} + \frac{\partial u}{\partial x} + \frac{\partial u}{\partial y} = 0,$$

for various initial conditions. Boundary condition is defined as the flux on domain boundary to be equal zero.

(1) ***Step:***

We started with the initial condition

$$u = \begin{cases} u = 0, & x < 0.5, \ \forall y, \\ u = 1, & x \geq 0.5, \ \forall y, \end{cases}$$

on a squared domain $[0, 1] \times [0, 1]$ (see Fig. 6.1).

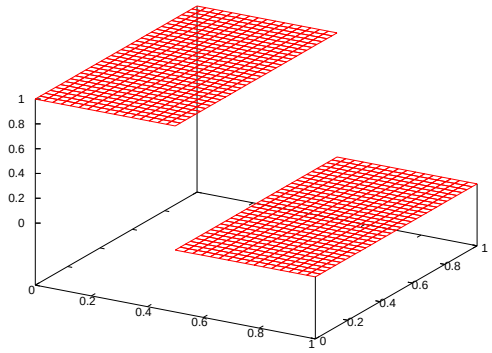

Figure 6.1: Figure show the initial condition for the test case.

In Fig. 6.2 and 6.3 we show the solution for different time steps for different method order. In Fig. 6.2 we have basis functions to be constant polynomials and in Fig. 6.3 we have basis functions to be linear polynomials.

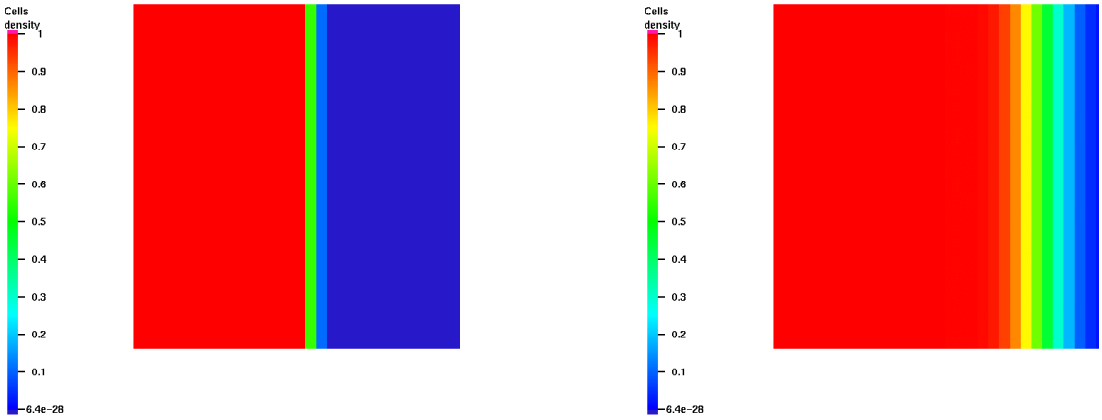

Figure 6.2: Figures show solutions with constant polynomials for different times.

(2) ***Square hill:***

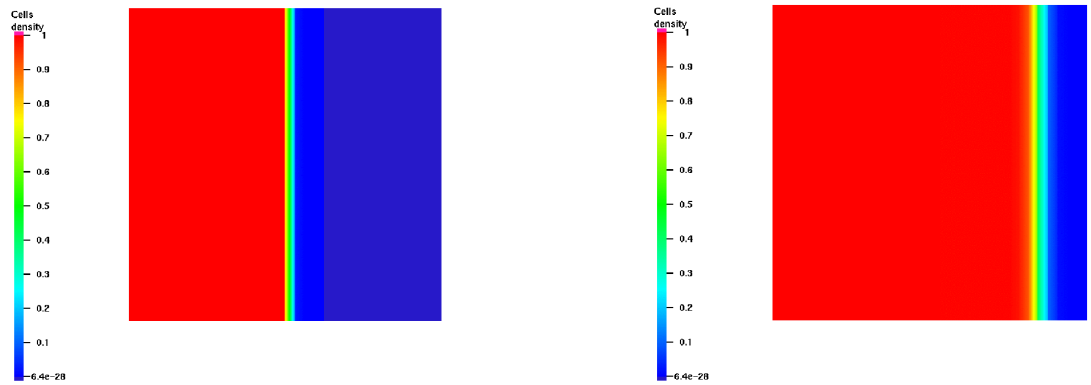

Figure 6.3: Figures show solutions with linear polynomials for different times.

By the square hill we mean initial condition as

$$u = \begin{cases} u = 1, & x \in [0.1, 0.3] \wedge y \in [0.1, 0.3], \\ u = 0, & \text{else}, \end{cases}$$

on a squared domain $[0, 1] \times [0, 1]$ (see Fig. 6.4).

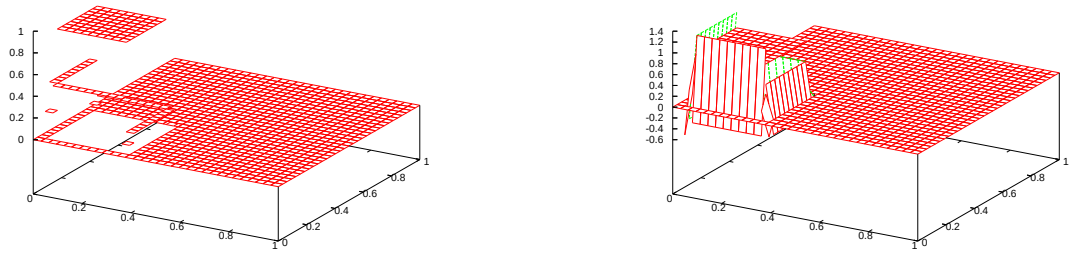

Figure 6.4: Figure show the initial condition for different polynomial orders (l=0, l=1).

In Figs. 6.5, 6.6, 6.7 we show results for the squared initial condition for different time steps and different polynomial orders. We have also included dynamic mesh adaption for the case of constant polynomials (Fig. 6.6).

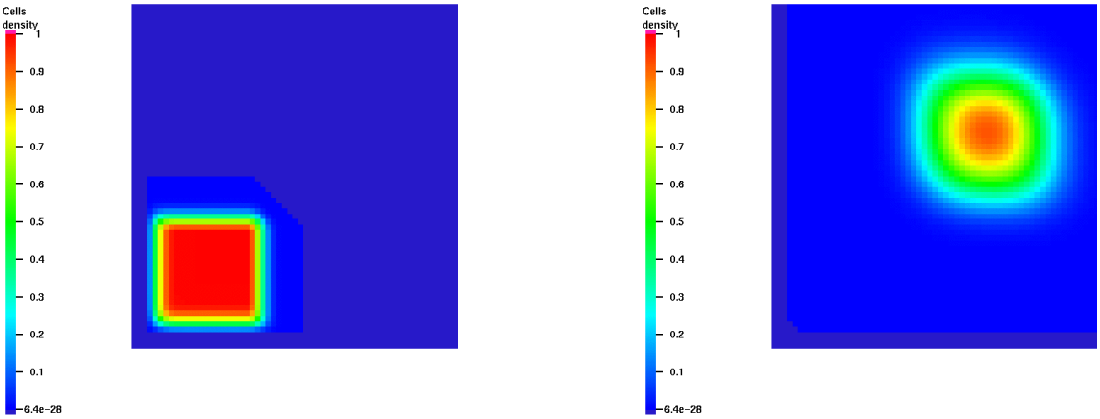

Figure 6.5: Figures show solutions with constant polynomials for different times.

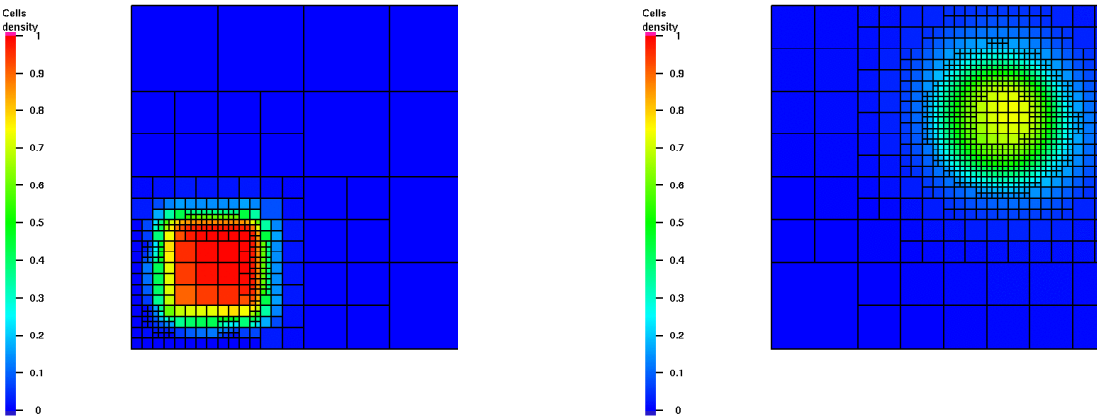

Figure 6.6: Figures show solutions with constant polynomials for different times with dynamics mesh addaption.

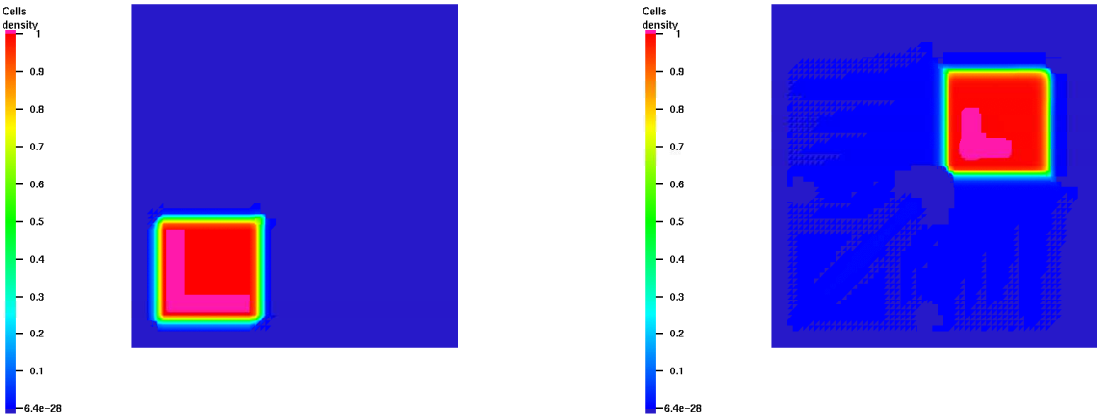

Figure 6.7: Figures show solutions with linear polynomials for different times.

We observe that constant polynomials have quite high numerical dissipation, comparing to the linear or first oder polynomial basis functions. We can improve results including dynamic mesh adaption. Anyhow, Deal.II library does not completely support the dynamic mesh addaption. For the computational speed, would be nice to have support for dynamic polynomial addaption, i.e. where a solution is not changing much, we could use the lower order basis or higher order basis over very large cell. However, we must pay attention near the discontinuities, where the most accurate solution is obtained with constant polynomials.

6.3.2 Anti planar case

We will now procede with the simulations of the model (6.6). The condition of yielding is defined by equation (6.5). Initially, we start with a small perturbation of angle α over the diagonal line in square domain $[-1,1] \times [-1,1]$. Line will not extend from corner to corner, but inside the 3/4 of the diagonal. This will cause to start a formation of the shear band. Boundary condition was defined as the flux trough the boundary is equal to 0. The step in time integration was calculated in each time step to ensure the L^2 stability.

$$|c|\frac{\Delta t}{\Delta x} \leq CFL_{L^2},$$

where in [CS90] show that

$$CFL_{L^2} = \frac{1}{2k+1},$$

with k being the order of used polynomials.

The initial condition for stress is equal to 0, and velocity has a stationary linear profile

$$v(x,y,t=0) = 0.04x, \quad \tau_1(x,y,t=0) = 0.0, \quad \tau_2(x,y,t=0) = 0.0.$$

In the next figures we show results of simulation for the final time. Beyond this time the solution blows up.

In Figs. 6.8, 6.9, 6.10 and 6.11 we show simulation results for the longest time possible, before the blowup occurs. We observe that longer simulation times were obtained with the use of mesh adaptivity. This shows, that the solution of this

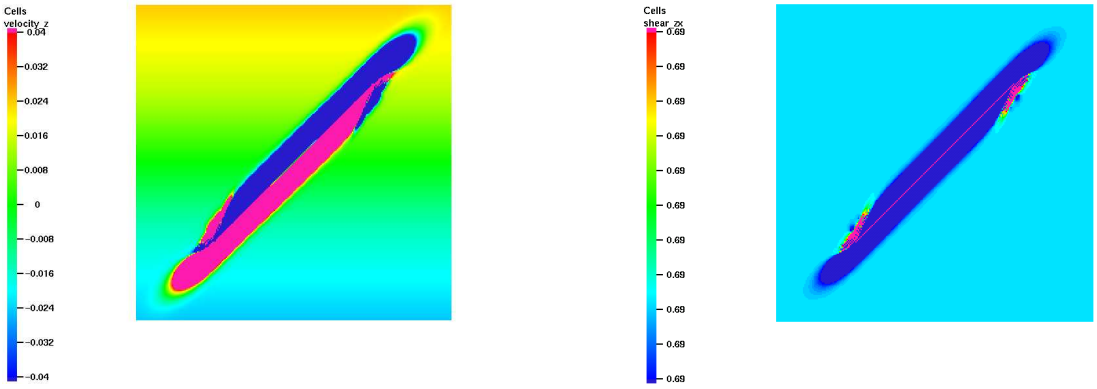

Figure 6.8: 0^{th} order, grid 256x256, $t = 3\,10^{-5}$; left-v, right-τ_1.

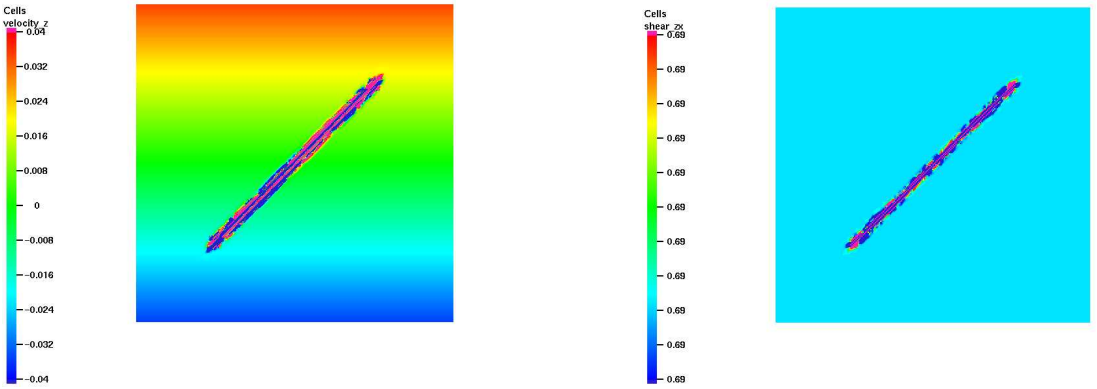

Figure 6.9: 1^{th} order, grid 256x256, $t = 3\,10^{-5}$; left-v, right-τ_1.

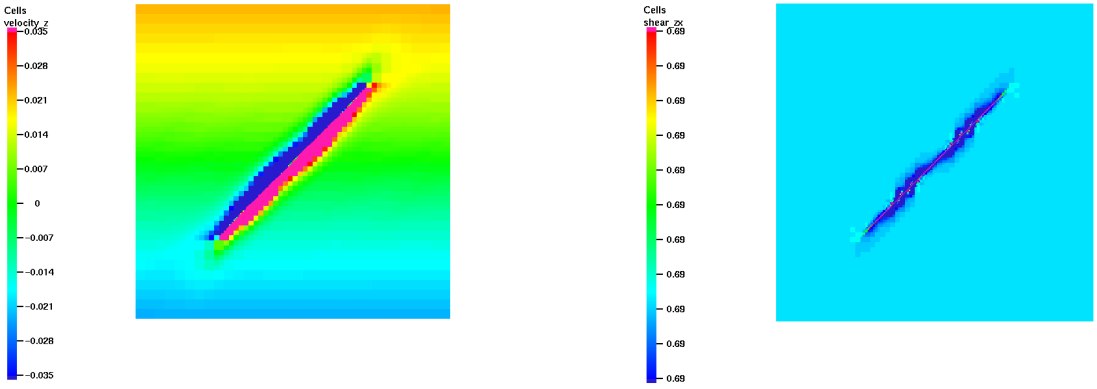

Figure 6.10: 0^{th} order, adaptive grid, $t = 5\,10^{-5}$; left-v, right-τ_1.

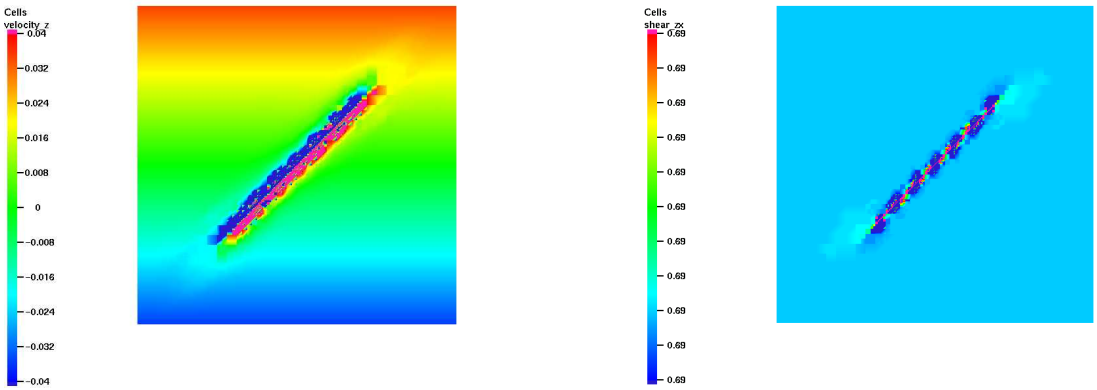

Figure 6.11: 1^{th} order, adaptive grid, $t = 5\,10^{-5}$; left-v, right-τ_1.

model is mesh dependent and good adaptivity algorithm would help much in the computation of solutions.

Results were compared qualitatively with [GT98] and they are in a good agreement.

Chapter 7

Conclusion

In this thesis we have considered theoretical and numerical investigations of the slow dense granular flow (powder flow). The aim was to get familiar with the models and analyse them. Slow dense granular flow models are part of the so called family of ***Generalised Newtonian Fluids***. SDGF model is highly nonlinear in constitutive relation. This nonlinearty causes big problems in numerical analysis. With regular numerical methods, such problem can not be solved with prescribed accuracy. Advanced numerical techniques such as special preconditioners, smoothers, etc are needed.

As we said in the introduction there are many models of slow granular flow in the market today. In this thesis, we analysed models derived from plasticity theory, where yield condition and associated flow rule are used to derive constitutive relation.

First part of the thesis treat analytical investigation of the rigid-plastic model. In the beginning we investigate the 1D model. We can imagine it as a flow in a pipe, where radial and azimuthal changes are averaged. 1D model of incompressible flow showed trivial solution, rigid block motion. However, for the compressible type of flow we found that the system of PDE's is hyperbolic. For 2D model we derived the prototype nonlinear parabolic partial differential equation. The equation represents the incompressible type of flow in simple shear experiment. We found special solutions but all of them are unbounded due to the ill-posed nature of PDE. We showed that solving this PDE is hard task, probably mission impossible.

Second part of the thesis is devoted to the numerical analysis. We analysed two models, the rigid-plastic model and the elasto-plastic model.

Numerical investigation of the rigid-plastic model showed the same results as were predicted with the analysis in the part one of the thesis. We can take this

as a guarantee for the simplification we did in the derivation of the nonlinear parabolic PDE. Nonlinearities caused us headache when solving linear system of equation. In the full newton's method, iterative solver of the linear system did not converge not even for second newton iteration step. In the case of fixpoint method we could obtain desirous convergence accuracy of iterative solution of linear system just for one of solutions. We observed that solution is not unique. The research in existence and uniqueness of steady state models could be a nice topic for the future research. We could do the same variational analysis of quasi static rigid-plastic model without convective term (equation (2.43)) as was done in a book of Fuchs & Segerin [FS00].

The elasto-plastic model (6.3) has special property to describe just the shear stress of the stress tensor. It was derived by D.G. Schaeffer [Sch92] and is a perfect model to test new numerical ideas for slow dense granular flow. Elasto-plastic model was solved with the Discontinuous Galerkin - Runge Kutta finite element method with mesh adaptivity. We showed that mesh adaptivity helps much in the speed up of calculation. Results were compared with the results obtained in the work of Garaizar and Trangenstein [GT98]. We observe the same phenomena and conclude that this numerical algorithm can be a good choice for simulations of slow dense granular flow.

Appendix A

Vectors and Tensors

A.1 Vectors

A ***vector*** is an element of $\mathbb{R}^3$, which is real 3-dimensional inner product space. Vectors are denoted by the bold-face symbols.

- The ***dot product*** of vectors $\boldsymbol{a}$ and $\boldsymbol{b}$ is denoted $\boldsymbol{a} \cdot \boldsymbol{b}$
- The ***cross product*** of vectors $\boldsymbol{a}$ and $\boldsymbol{b}$ is denoted $\boldsymbol{a} \wedge \boldsymbol{b}$
- The ***basis*** for $\mathbb{R}^3$ is denoted $\boldsymbol{e}_1, \boldsymbol{e}_2, \boldsymbol{e}_3$. Then any vector $\boldsymbol{u}$ can be represented uniquely as a linear combination of these base vectors

$$\boldsymbol{u} = \sum_{i=1}^{3} u^i \boldsymbol{e}_i = u^i \boldsymbol{e}_i, \qquad \text{by Einstein summation convention}$$

- The ***norm*** of vector $\boldsymbol{a}$ is denoted $\|\boldsymbol{a}\|$

$$\|\boldsymbol{a}\| := \sqrt{\boldsymbol{a} \cdot \boldsymbol{a}}$$

A.2 Tensors

Elements of the 9-dimensional space $\mathrm{Lin} := \mathcal{L}(\mathbb{R}^3, \mathbb{R}^3)$ of linear transformation of $\mathbb{R}^3$ to itself are called (second-order) ***tensors***. We may call vectors first-order tensors and call scalars zero-order tensors. We denote second-order tensors by ***bold-face serif*** symbols. The value of a tensor $\mathbf{A}$ at vector $\boldsymbol{u}$ is the vector denoted by $\mathbf{A}\boldsymbol{u}$.

- The ***tensor product*** of vectors $\boldsymbol{u}$ and $\boldsymbol{v}$ is defined

$$\boldsymbol{u} \otimes \boldsymbol{v} = u^i v^j \boldsymbol{e}_i \otimes \boldsymbol{e}_j$$

  Tensor $\mathbf{A}$ can be written in the form of the tensor product

$$\mathbf{A} = A^{ij} \boldsymbol{e}_i \otimes \boldsymbol{e}_j$$

- The ***product*** of a tensors $\mathbf{A}$ and $\mathbf{B}$ is denoted $\mathbf{AB}$
- We define $\mathbf{A}^2 := \mathbf{AA}$, $\mathbf{A}^3 := \mathbf{AAA}$, etc.
- The ***transpose*** (or ***adjoint***) of $\mathbf{A}$ is denoted $\mathbf{A}^\mathsf{T}$

$$\boldsymbol{u} \cdot (\mathbf{A}\boldsymbol{v}) = (\mathbf{A}^\mathsf{T}\boldsymbol{u}) \cdot \boldsymbol{v}, \qquad \forall \boldsymbol{u}, \boldsymbol{v} \in \mathbb{R}^3$$

- $\mathbf{A}$ is called ***symmetric*** iff $\mathbf{A} = \mathbf{A}^\mathsf{T}$
- $\mathbf{A}$ is called ***antisymmetric*** or ***skew*** iff $\mathbf{A} = -\mathbf{A}^\mathsf{T}$
- Every tensor $\mathbf{A}$ has a unique decomposition as a sum of a symmetric and skew tensor:

$$\mathbf{A} = \frac{1}{2}(\mathbf{A} + \mathbf{A}^\mathsf{T}) + \frac{1}{2}(\mathbf{A} - \mathbf{A}^\mathsf{T})$$

- The ***tensor dot product*** of a tensors $\mathbf{A}$ and $\mathbf{B}$ is denoted $\mathbf{A} : \mathbf{B}$

$$\mathbf{A} : \mathbf{B} = \mathbf{B} : \mathbf{A}$$

- The ***trace*** of a tensor $\mathbf{A}$ is denoted $\mathsf{tr}\mathbf{A}$

$$\mathsf{tr}\mathbf{A} := \mathbf{A} : \mathbf{I} = \mathbf{I} : \mathbf{A}$$

$$\mathsf{tr}(\mathbf{A}\mathbf{B}^\mathsf{T}) := \mathbf{A} : \mathbf{B}$$

- The ***norm*** of a tensor $\mathbf{A}$ is defined $\|\mathbf{A}\|$

$$\|\mathbf{A}\| := \sqrt{\mathbf{A} : \mathbf{A}} = \sqrt{\mathsf{tr}(\mathbf{A}\mathbf{A}^\mathsf{T})}$$

- Corresponding to arbitrary tensor $\mathbf{A}$, there are scalars $\mathrm{I}_\mathbf{A}$, $\mathrm{II}_\mathbf{A}$, $\mathrm{III}_\mathbf{A}$ such that

$$\begin{aligned} \mathrm{I}_\mathbf{A} &:= \mathsf{tr}\mathbf{A} \\ \mathrm{II}_\mathbf{A} &:= \frac{1}{2}\left[(\mathsf{tr}\mathbf{A})^2 - \mathsf{tr}(\mathbf{A}\mathbf{A}^\mathsf{T})\right] \\ \mathrm{III}_\mathbf{A} &:= \mathsf{det}\mathbf{A} \end{aligned}$$

  These scalars are called the ***principal invariants*** of a tensor $\mathbf{A}$.

- Every tensor $\mathbf{A}$ has a unique decomposition as a sum of a ***spherical tensor*** $\overset{\circ}{\mathbf{A}}$ and ***deviatoric tensor*** $\overset{*}{\mathbf{A}}$:

$$\mathbf{A} = \overset{\circ}{\mathbf{A}} + \overset{*}{\mathbf{A}} = \frac{1}{3}\,\mathrm{I}_{\mathbf{A}}\,\mathbf{I} + \overset{*}{\mathbf{A}}$$

We have next relations for spherical and deviatoric tensor

$$\begin{aligned}
\mathrm{I}_{\overset{\circ}{\mathbf{A}}} &= \mathrm{I}_{\mathbf{A}} \\
\mathrm{II}_{\overset{\circ}{\mathbf{A}}} &= \frac{1}{3}\,\mathrm{I}_{\mathbf{A}}^2 \\
\mathrm{I}_{\overset{*}{\mathbf{A}}} &= 0 \\
\mathrm{II}_{\overset{*}{\mathbf{A}}} &= \mathrm{II}_{\mathbf{A}} - \frac{1}{3}\,\mathrm{I}_{\mathbf{A}}^2
\end{aligned}$$

Bibliography

[Bat67] G. K. Batchelor, ***An introduction to fluid dynamics***, Cambridge University Press, 1967.

[BHK] Wolfgang Bangerth, Ralf Hartmann, and Guido Kanschat, ***deal.ii differential equations analysis library, technical reference***, IWR, `http://www.dealii.org`.

[BP02] N. J. Balmforth and A. Provenzale, ***Selected topics in geoleogical and geomorphological fluid mechanics***, Springer, 2002.

[Cou76] C. A. Coulomb, ***Essai sur une application des regles de maximis et minimis a quelques problemes de statique, relatifs a l'architecture***, Memoires de Mathematique de l'Academie Royale des Sciences (Paris) **7** (1776), 343–382.

[CS89a] B. Cockburn and Chi-Wang Shu, ***Tvb runge-kutta local projection discontinuous galerkin finite element method for conservation laws - general framework***, Mathematics of Computation **52** (1989), no. 186, 411–435.

[CS89b] ———, ***Tvb runge-kutta local projection discontinuous galerkin finite element method for conservation laws - one-dimensional system***, Journal of Computational Physics **84** (1989), 90–113.

[CS90] ———, ***Tvb runge-kutta local projection discontinuous galerkin finite element method for conservation laws - the multydimensional case***, Mathematics of Computation **54** (1990), no. 190, 545–581.

[DP52] D. C. Drucker and W. Prager, ***Soil mechanics and plastic analysis or limit design***, Quatterly of Applied Mathematics **10** (1952), 157–165.

[FS00] Martin Fuchs and Gregory Segerin, ***Variational methods for problems from plasticity theory and for generalised newtonian fluids***, Lecture notes in mathematics - 1794, Springer, 2000.

[GM01] P. Gremaud and J. V. Matthews, ***On the computation of steady hopper flows: I, stress determinatio for coulomb materials***, NCSU-CRSC Tech Report CRSC-TR99-35, University of North Carolina, 2001.

[GT98] F. X. Garaizar and J. Trangenstein, ***Adaptive mesh refinement and front tracking for shear bands in an antiplane shear model***, SIAM J.Sci.Cmp. **20** (1998), no. 2, 750–779.

[Gur81] M. E. Gurtin, ***An introduction to continuum mechanics***, Academic Press, 1981.

[Han05] Shaum Handy, ***Towards a theory of granular plasticity***, J. Eng. Math. **52** (2005), no. 1, 137–146.

[Har01] D. Harris, ***Ill and well posed models of granular flow***, Acta. Mech. **146** (2001), 199–225.

[Hul91] M. A. Hulsen, ***The discontinuous galerkin method with explicite runge-kutta time integration for hyperbolic and parabolic system with source term***, Laboratory for Aero and Hydrodynamics MEMT 19, Delft University of Technology, Netherlands, 1991.

[Kev00] J. Kevorkian, ***Partial differential equation; analytical solution techniques***, Springer, 2000.

[Lub90] J. Lubliner, ***Plasticity theory***, Macmillian Publishing, 1990.

[MC72] M. M. Mehrabadi and S. C. Cowin, ***Stress-strain behaviour of soils***, Henley:Foulis, 1972.

[MH92] J. E. Marsden and T. J. R. Hughes, ***Mathematical foundation of elasticity***, Dover, 1992.

[MS04] J. M. Matthews and D. G. Schaeffer, ***A well-posed free boundary value problem for a hyperbolic equation with dirichlet boundary conditions***, SIAM J. Math. Anal. **36** (2004), 256–271.

[Ned92] R. M. Nedderman, ***Statics and kinematics of granular materials***, Cambridge University Press, New York, 1992.

[Oua05] Abderrahim Ouazzi, ***Finite element simulation of nonlinear fluids with application to granular material and powder***, Ph.D. thesis, Fachbereich Mathematik, Universitat Dortmund, 2005.

[PS87] E. B. Pitman and D. G. Schaeffer, ***Stability of time dependant compressible granular flow in two dimensions***, Communications on Pure and Applied Mathematics **40** (1987), 421–447.

[Sch87] D. G. Schaeffer, ***Instability in the evolution equations describing incompressible granular flow***, Journal of Differential Equations **66** (1987), no. 1, 19–50.

[Sch92] ———, ***A mathematical model for localization in granular flow***, Proc. R. Soc. Lond. A **436** (1992), 217–250.

[Spe64] A. J. M. Spencer, ***A theory of kinematics of ideal solids under plane strain condition***, J. Mech. Phys. Solids **12** (1964), 337–351.

[Spe86] ———, ***Instability of stedy flow of granular materials***, Acta. Mech. **64** (1986), 77–87.

[SSP90] D. G. Schaeffer, M. Shearer, and E.B. Pitman, ***Instability in critical state theories of granular flow***, SIAM J. Appl. Math. **50** (1990), no. 1, 33–47.

[SSW06] D. G. Schaeffer, M. Shearer, and T. P. Witelski, ***Boundary-value problems for hyperbolic pde related to steady granular flow***, Physica D **11** (2006).

[SW68] A. Schofield and C. Worth, ***Critical state soil mechanics***, McGraw-Hill Publishing, 1968.

[TMT02] G. I. Tardos, S. McNamara, and I. Talu, ***Slow and intermediate flow of a frictional bulk powder in the couette geometry***, Powder Technology **4686** (2002), 1–17.

[TT65] C. Truesdell and R. A. Toupin, ***The classical field theories***, Springer-Verlag, 1965.

[VG85] I. Vardulakis and B. Graf, ***Calibration of constitutive models for granular materials using data from biaxial experiments***, Geotechnique **35** (1985), 299–317.

[WSS01] T. P. Witelski, D. G. Schaeffer, and M. Shearer, ***A discrete model for an ill-posed nonlinear parabolic pde***, Mathematics and Mechanics of Solids **160** (2001), 189–221.

Curriculum Vitae

24.Dec.1972	*Born* in Koper, Slovenia
1978 - 1986	*Primary School* "OŠ Janka Premrla - Vojka" Koper, Slovenia
1986 - 1990	*Secondary Navy School* "SPPŠ Piran" Portorož, Slovenia
1990 - 1992	Ocean going navigation as junior officer
1992 - 1994	*Diploma in Navigation*, Faculty of Maritime Engineering University of Ljubljana, Slovenia
1994 - 2001	*Diploma in Physics*, Faculty of Mathematics and Physics University of Ljubljana, Slovenia
2002 - 2003	*Master in Modelling of complex realities*, Joint ICTP/SISSA Trieste, Italy
2003 - 2006	*PhD in Applied Mathematics*, Department of Mathematics TU Kaiserslautern, Germany